Real Stueckelberg Quantum Geometry and Unbroken Supersymmetry in the Rotating Shallow Water Model

Andrei Galiautdinov *

Posted Date: 20 May 2026

doi: 10.20944/preprints202605.0606.v2

Keywords: topological fluid dynamics; rotating shallow water model; rotating shallow water equations (RSWE); equatorial waves; Coriolis parameter; Kelvin and Yanai modes; Poincare waves; Rossby waves; Stueckelberg real quantum mechanics; real Hilbert space; Fubini-Study metric; Berry phase; Berry connection; Berry curvature; Chern numbers; supersymmetry (SUSY); supersymmetric quantum mechanics (SUSY QM); momentum-dependent chiral grading operator; Witten index

 doi:10.20944/preprints202605.0606.v2

Article

Real Stueckelberg Quantum Geometry and Unbroken Supersymmetry in the Rotating Shallow Water Model

Andrei Galiautdinov

Department of Physics and Astronomy, University of Georgia, Athens, Georgia 30602, USA; ag1@uga.edu

Abstract

The topological properties of planetary fluids are typically analyzed by mapping classical fluid equations onto complex quantum mechanical models. Here we present a purely real, six-dimensional Stueckelberg quantum mechanical formulation of the rotating shallow water equations to demonstrate that these topological features are intrinsic to the classical kinematics itself. Operating entirely within $\mathbb{R}^6$ we decouple the complex quantum geometric tensor into an independent real Fubini-Study metric and a real antisymmetric Berry curvature. Our real-variable approach explicitly derives a topological magnetic monopole of charge $C = -2$ and captures the inherent scale invariance of the fluid's geometry without explicit complex coordinate representation. We suggest that continuous variations in the Coriolis parameter model the adiabatic geometric evolution of the Archean Earth, and we propose a laboratory rotating-tank experiment to physically measure this parameter sweep. Finally, we show that our real 6D formulation naturally maps to unbroken supersymmetric quantum mechanics. By identifying a purely real supercharge and calculating a fluid Witten index of $W = -2$, we demonstrate a strict mathematical symmetry between the topological charge of the propagating bands and the invariant of the unbroken zero-energy geostrophic vacuum. We advance the mathematically supported viewpoint that steady-state geostrophic weather patterns represent the exact supersymmetric ground states of the rotating fluid system. Consequently, the topological isolation of this vacuum naturally restricts the spectral flow across the equator, providing a theoretical explanation for the unidirectional eastward motion of equatorial boundary waves.

Keywords: topological fluid dynamics; rotating shallow water model; rotating shallow water equations (RSWE); equatorial waves; Coriolis parameter; Kelvin and Yanai modes; Poincare waves; Rossby waves; Stueckelberg real quantum mechanics; real Hilbert space; Fubini-Study metric; Berry phase; Berry connection; Berry curvature; Chern numbers; supersymmetry (SUSY); supersymmetric quantum mechanics (SUSY QM); momentum-dependent chiral grading operator; Witten index

1. Introduction

In recent years concepts from topological band theory originally developed in solid-state physics [1,2] have been applied to classical fluids. In planetary oceans and atmospheres the planet's rotation breaks time-reversal symmetry, creating a frequency gap between slow geostrophic weather patterns and fast gravity waves. As established by Delplace *et al.* [3] (also [4,5]), building upon the foundational work by Matsuno [6], this gap topologically guarantees the emergence of boundary states, such as equatorial Kelvin waves [7], which are forced to travel in only one direction along the equator.

To analyze these phenomena, standard models intrinsically rely on mapping classical equations into complex mathematical spaces, a technique adopted in classical topological mechanics and acoustics [8,9]. Of particular importance to us is the recent work by Ganeshan and Dorsey [10], who map the rotating shallow water equations to a complex pseudo-spin-1 system in an artificial magnetic field. Since this theoretical approach bypasses the fact that classical fluids are fundamentally real, a natural question arises as to whether a comparable, yet fully real, formulation of the rotating shallow water model is possible. This question was anticipated in the commentary by Biello and Dimofte

 doi:10.20944/preprints202605.0606.v2

[11] accompanying the original paper by Delplace *et al.* [3], which noted that relying on complex wavefunctions leaves open conceptual issues, such as, e. g., whether topological winding numbers simply cancel out when combining them to form real-valued physical waves.

In this paper we propose an approach based on a purely real, six-dimensional Stueckelberg formulation of quantum mechanics [12]. By keeping all calculations within $\mathbb{R}^6$ we show that the topological features of planetary waves emerge directly from the classical equations, without requiring complex variables.

We construct the purely real formulation of the quantum geometric tensor [13–17] and extract its two independent real parts: a symmetric Fubini-Study metric [18,19] and an antisymmetric Berry curvature [20]. Using real components we re-derive a topological magnetic monopole with a charge of $C = -2$. This demonstrates that real classical superpositions do not suffer from topological cancellation; the winding arises from the real symplectic kinematics of the fluid, rather than an imaginary phase, with the negative sign explicitly dictating the chirality of the spectral flow.

We connect our formulation to planetary evolution by treating the continuous variation of the rotation parameter f as analogous to conditions on the Archean Earth, which rotated significantly faster. We outline a laboratory rotating tank experiment designed to gradually decelerate, providing a practical method to measure these geometric changes in real time.

Next, we show that our real 6D model shares the mathematical structure of supersymmetric quantum mechanics (SUSY QM) [21–25]. Within this interpretation the main dynamical Hamiltonian, $\mathcal{H}_S$ (for Stueckelberg), of the rotating shallow water equations acts as a purely real supercharge, $\mathcal{Q} = \mathcal{H}_S$, while the formal supersymmetric Hamiltonian is generated by its square, $\mathcal{H}_{SUSY} = \mathcal{Q}^2$. By introducing a momentum-dependent chiral grading operator that partitions the fluid into its divergent and rotational Helmholtz components we calculate a Witten index of $W = -2$.[1] The exact structural alignment between the topological monopole charge $C = -2$ and the Witten index $W = -2$ demonstrates that the topological invariant of the high-frequency propagating bands perfectly mirrors the invariant of the unbroken zero-energy geostrophic vacuum. Rather than indicating two distinct physical phenomena, this integer protects a doubly degenerate zero-frequency subspace, corresponding to the orthogonal sine and cosine spatial quadratures of a single continuous geostrophic balance. This guarantees the stability of large-scale geostrophic weather patterns on a rotating planet. Furthermore, this unbroken classical vacuum structure fulfills the topological role traditionally played by a filled Fermi sea in quantum systems. Its topological isolation restricts the spectral flow across the equator, naturally forcing the observed boundary states to propagate exclusively eastward.

Additionally, to explicitly demonstrate how this bulk topology governs the physical fluid boundaries, in Appendix A we re-derive Matsuno's equatorial edge states (the Kelvin and Yanai waves) entirely within our real Stueckelberg formulation. In Appendix B, we outline the proof of Witten's theorem in the finite-dimensional real Hilbert space, and in Appendix C, for completeness, we provide the supersymmetric formulation in the standard complex-valued description of the rotating shallow water model. Finally, in Appendix D, we review the mathematical foundations of topological winding and higher-dimensional Chern numbers, establishing how these global invariants manifest as macroscopic energy allocations in real-valued classical fluids. To overcome the counter-intuitive nature of degree-two mappings, we outline three equivalent geometric perspectives (adapted from standard literature in algebraic topology [27], complex analysis [28], and topological vector field theory [1,29]) to visualize how a state space can smoothly envelop a singularity twice. We culminate this with an explicit, real-variable analytical derivation using the upper Poincar'e (P_1) mode as an example, reveal-

[1] Recently, Tong [26] provided a complementary perspective by reformulating the rotating shallow water equations as a macroscopic $2+1$-dimensional Abelian gauge theory. In that approach the kinematic differences between the scalar height and vector velocity fields are mapped to magnetic and electric fields, respectively. This models linearised Poincaré waves via Maxwell-Chern-Simons theory and identifies coastal Kelvin waves as chiral gauge edge modes. While Tong exposes the fluid's topological nature via a continuous real-space effective field theory, and Ganeshan & Dorsey [10] do so via momentum-space Berry curvature, our 6D real formulation reveals the exact same underlying reality through a local algebraic description via supersymmetric quantum mechanics and the Witten index.

 doi:10.20944/preprints202605.0606.v2

ing how clearing the origin's coordinate singularity naturally produces the double-angle harmonics and demonstrating that the singular core is anchored by a symmetric, circularly polarized inertial oscillation.

2. Real Quantum Geometry via Stueckelberg Formalism

The usual derivations of the quantum geometric tensor rely on a complex Hilbert space. Because macroscopic classical fluid fields are real-valued quantities, we apply the 1960 method by Stueckelberg [12], which showed that quantum mechanics can be alternatively formulated over a real Hilbert space. This is achieved by introducing an antisymmetric super-selection operator J satisfying the algebraic condition $J^2 = -I$.

2.1. Rotating Shallow Water System and Dispersion Relations

The rotating shallow water equations (RSWE) that describe the dynamics of a thin layer of fluid (of height $h(\boldsymbol{x}, t)$ and horizontal velocity $\boldsymbol{u}(\boldsymbol{x}, t) = (u, v)$) on a two-dimensional surface have the form [30,31],

$$\partial_t h + \nabla \cdot (h\boldsymbol{u}) = 0, \quad \partial_t \boldsymbol{u} + (\boldsymbol{u} \cdot \nabla)\boldsymbol{u} = -g\nabla h - f\hat{\boldsymbol{n}} \times \boldsymbol{u}, \tag{1}$$

where $u(\boldsymbol{x}, t)$ and $v(\boldsymbol{x}, t)$ represent the zonal and meridional horizontal velocity anomalies,

$$f = 2\Omega \sin \vartheta \tag{2}$$

is the Coriolis parameter (with ϑ being the latitude measured from the equator), g denotes the gravitational acceleration, and $\hat{\boldsymbol{n}}$ is the local vertical unit vector. The state of the fluid system may be conveniently described by a real three-dimensional vector field,

$$\Psi(\boldsymbol{x}, t) = (u, v, \eta)^T = \begin{pmatrix} u \\ v \\ \eta \end{pmatrix}, \tag{3}$$

where

$$\eta(\boldsymbol{x}, t) = [h(\boldsymbol{x}, t) - H]/H \tag{4}$$

represents the free-surface height anomaly, with H being the mean depth of the unperturbed fluid. Following standard dimensional re-scaling [3] (also [10]) we define the non-dimensionalized variables (denoted with tildes),

$$v = c\tilde{v}, \quad u = c\tilde{u}, \quad \eta = H\tilde{\eta}, \quad x = L_d\tilde{x}, \quad y = L_d\tilde{y}, \quad t = \frac{\tilde{t}}{2\Omega}, \quad f = 2\Omega\tilde{f}, \tag{5}$$

where the characteristic velocity and length scales of the fluid system are defined by

$$c^2 = gH, \quad L_d = \frac{c}{2\Omega}. \tag{6}$$

Dropping the tildes for notational simplicity the *linearized RSWE* take the form,

$$\partial_t \Psi = L_{\text{sp}}\Psi, \tag{7}$$

where

$$L_{\text{sp}} = \begin{pmatrix} 0 & f & -\partial_x \\ -f & 0 & -\partial_y \\ -\partial_x & -\partial_y & 0 \end{pmatrix} \tag{8}$$

is the real spatial differential operator.

 doi:10.20944/preprints202605.0606.v2

We next construct an explicitly real propagating plane wave solution to the fluid equations as a superposition of two quadratures,

$$\Psi(\boldsymbol{x},t) = \Psi_1(\boldsymbol{k})\cos(\boldsymbol{k}\cdot\boldsymbol{x} - \omega(\boldsymbol{k})t) + \Psi_2(\boldsymbol{k})\sin(\boldsymbol{k}\cdot\boldsymbol{x} - \omega(\boldsymbol{k})t), \tag{9}$$

where $\Psi_1(\boldsymbol{k})$ and $\Psi_2(\boldsymbol{k})$ are appropriately chosen three-dimensional real column vectors. Substituting into Eq. (7) and using (8), after some algebra, we find the system,

$$\omega(\boldsymbol{k})\Psi_1 = -K\Psi_1 + F\Psi_2, \quad -\omega(\boldsymbol{k})\Psi_2 = F\Psi_1 + K\Psi_2, \tag{10}$$

with

$$F = \begin{pmatrix} 0 & f & 0 \\ -f & 0 & 0 \\ 0 & 0 & 0 \end{pmatrix} = -F^{\mathrm{T}}, \quad K = \begin{pmatrix} 0 & 0 & -k_x \\ 0 & 0 & -k_y \\ -k_x & -k_y & 0 \end{pmatrix} = K^{\mathrm{T}}, \tag{11}$$

which may be re-written in the 6×6 matrix form,

$$\begin{pmatrix} F & K \\ -K & F \end{pmatrix}\begin{pmatrix} \Psi_1 \\ \Psi_2 \end{pmatrix} = \omega(\boldsymbol{k})\begin{pmatrix} 0 & -I_3 \\ I_3 & 0 \end{pmatrix}\begin{pmatrix} \Psi_1 \\ \Psi_2 \end{pmatrix}. \tag{12}$$

Defining the 6×6 matrices,

$$\mathcal{G} = \begin{pmatrix} F & K \\ -K & F \end{pmatrix}, \quad \mathcal{J} = \begin{pmatrix} 0 & -I_3 \\ I_3 & 0 \end{pmatrix}, \tag{13}$$

we see that

$$\mathcal{J}^{\mathrm{T}} = -\mathcal{J}, \quad \mathcal{J}^2 = -I_6, \quad \mathcal{G}^{\mathrm{T}} = -\mathcal{G}, \quad [\mathcal{G},\mathcal{J}] = 0, \tag{14}$$

with $\mathcal{J}$ functioning as the imaginary unit i, and $\mathcal{G}$ being antisymmetric. Multiplying by $(-\mathcal{J})$ on the left, Eq. (12) becomes

$$\mathcal{M}\begin{pmatrix} \Psi_1 \\ \Psi_2 \end{pmatrix} = \begin{pmatrix} 0 \\ 0 \end{pmatrix}, \tag{15}$$

with

$$\mathcal{M} = \begin{pmatrix} -K-\omega(\boldsymbol{k}) & F \\ -F & -K-\omega(\boldsymbol{k}) \end{pmatrix} = \begin{pmatrix} -\omega(\boldsymbol{k}) & 0 & k_x & 0 & f & 0 \\ 0 & -\omega(\boldsymbol{k}) & k_y & -f & 0 & 0 \\ k_x & k_y & -\omega(\boldsymbol{k}) & 0 & 0 & 0 \\ 0 & -f & 0 & -\omega(\boldsymbol{k}) & 0 & k_x \\ f & 0 & 0 & 0 & -\omega(\boldsymbol{k}) & k_y \\ 0 & 0 & 0 & k_x & k_y & -\omega(\boldsymbol{k}) \end{pmatrix}, \tag{16}$$

whose determinant is

$$\det(\mathcal{M}) = \omega(\boldsymbol{k})^2(k_x^2 + k_y^2 + f^2 - \omega(\boldsymbol{k})^2)^2, \tag{17}$$

resulting in the dispersion relations for the three frequency bands,

$$\omega_0(\boldsymbol{k}) = 0, \quad \omega_+(\boldsymbol{k}) = \omega, \quad \omega_-(\boldsymbol{k}) = -\omega, \tag{18}$$

where

$$\omega \equiv +\sqrt{k_x^2 + k_y^2 + f^2}. \tag{19}$$

2.2. Connection to Stueckelberg's real Hilbert Space Formulation

The emergence of the 6×6 algebraic system in Eq. (12) reveals a deep structural isomorphism between the classical fluid dynamics and Ernst Stueckelberg's formulation of quantum mechanics in a

 doi:10.20944/preprints202605.0606.v2

real Hilbert space. Stueckelberg demonstrated that the imaginary unit i is not necessary for formulating quantum theory, provided the real state space is equipped with a distinguished, antisymmetric, orthogonal operator $\mathcal{J}$ satisfying $\mathcal{J}^2 = -I$.

In our approach the real six-dimensional state vector Φ is constructed by stacking the two spatial quadratures,

$$\Phi(\boldsymbol{k}) = \begin{pmatrix} \Psi_1(\boldsymbol{k}) \\ \Psi_2(\boldsymbol{k}) \end{pmatrix}. \tag{20}$$

Because Ψ_1 and Ψ_2 act as the real and imaginary parts of a conventional complex wave amplitude, applying the operator $\mathcal{J}$ physically rotates the quadratures by $\pi/2$, mimicking the algebraic operation of multiplying a complex state by i.

In standard complex quantum mechanics, time evolution is generated by a Hermitian Hamiltonian via the Schrödinger equation,

$$i\partial_t \psi = H\psi. \tag{21}$$

In Stueckelberg's real formalism the time evolution is instead governed by an antisymmetric generator of rotations in the real vector space. Returning to Eq. (12), we have,

$$\mathcal{G}\Phi = \omega(\boldsymbol{k})\mathcal{J}\Phi. \tag{22}$$

By multiplying both sides from the left by $(-\mathcal{J})$ and using $\mathcal{J}^2 = -I_6$ we obtain the purely real, symmetric eigenvalue problem,

$$\mathcal{H}_S\Phi = \omega(\boldsymbol{k})\Phi, \tag{23}$$

where $\mathcal{H}_S$ is the real Stueckelberg Hamiltonian defined by

$$\mathcal{H}_S \equiv -\mathcal{J}\mathcal{G} = \begin{pmatrix} 0 & I_3 \\ -I_3 & 0 \end{pmatrix}\begin{pmatrix} F & K \\ -K & F \end{pmatrix} = \begin{pmatrix} -K & F \\ -F & -K \end{pmatrix} = \begin{pmatrix} 0 & 0 & k_x & 0 & f & 0 \\ 0 & 0 & k_y & -f & 0 & 0 \\ k_x & k_y & 0 & 0 & 0 & 0 \\ 0 & -f & 0 & 0 & 0 & k_x \\ f & 0 & 0 & 0 & 0 & k_y \\ 0 & 0 & 0 & k_x & k_y & 0 \end{pmatrix}. \tag{24}$$

Recalling that $K^{\mathrm{T}} = K$ and $F^{\mathrm{T}} = -F$, we find,

$$\mathcal{H}_S^{\mathrm{T}} = \begin{pmatrix} -K^{\mathrm{T}} & -F^{\mathrm{T}} \\ F^{\mathrm{T}} & -K^{\mathrm{T}} \end{pmatrix} = \begin{pmatrix} -K & F \\ -F & -K \end{pmatrix} = \mathcal{H}_S, \tag{25}$$

verifying that $\mathcal{H}_S$ is symmetric, making it the exact real-space equivalent of a complex Hermitian Hamiltonian. We can now recognize that the matrix $\mathcal{M}$ in Eq. (15) is simply

$$\mathcal{M} = \mathcal{H}_S - \omega(\boldsymbol{k})I_6, \tag{26}$$

confirming that finding the null space of $\mathcal{M}$ is physically identical to finding the real eigenvectors of the Stueckelberg Hamiltonian.

Following Stueckelberg, we equip our finite-dimensional real space with the standard symmetric Euclidean inner product,

$$\langle \Phi_A, \Phi_B \rangle_{\mathbb{R}} = \Phi_A^{\mathrm{T}}\Phi_B = \sum_{j=1}^{6} (\Phi_A)_j (\Phi_B)_j. \tag{27}$$

Because we have scaled our physical variables with $c^2 = gH$ this real Euclidean metric corresponds to the total conserved mechanical energy of the fluid anomalies. Furthermore, Stueckelberg proved that

 doi:10.20944/preprints202605.0606.v2

the geometry of the standard complex inner product is entirely recoverable from this real metric via the relation,

$$\langle A_{\mathbb{C}}|B_{\mathbb{C}}\rangle_{\mathbb{C}} = \langle \Phi_A, \Phi_B\rangle_{\mathbb{R}} - i\langle \Phi_A, \mathcal{J}\Phi_B\rangle_{\mathbb{R}}, \tag{28}$$

where $|A_{\mathbb{C}}\rangle$ and $|B_{\mathbb{C}}\rangle$ are the corresponding complex-valued quantum states. Thus, our six-dimensional real Hilbert space preserves all quantum and geometric information without explicit complex coordinate representation.

To formalize this mathematical equivalence, we state the following:

Proposition 1. *The real Stueckelberg Hilbert space* $(\mathbb{R}^6, \langle\cdot,\cdot\rangle_{\mathbb{R}}, \mathcal{J})$ *is canonically isomorphic to the complex Hilbert space* $\mathbb{C}^3$ *equipped with the standard Hermitian inner product.*

Proof. Let $\Phi, \Psi \in \mathbb{R}^6$. We define scalar multiplication over the field of complex numbers by mapping the imaginary unit i to the action of the complex structure operator,

$$(a + ib)\Phi \equiv a\Phi + b\mathcal{J}\Phi. \tag{29}$$

Because $\mathcal{J}^2 = -I_6$, this multiplication satisfies the field axioms of $\mathbb{C}$. Furthermore, we define the mapping to the complex inner product as

$$\langle \Phi, \Psi\rangle_{\mathbb{C}} = \langle \Phi, \Psi\rangle_{\mathbb{R}} - i\langle \Phi, \mathcal{J}\Psi\rangle_{\mathbb{R}}. \tag{30}$$

Because the real Euclidean inner product $\langle\cdot,\cdot\rangle_{\mathbb{R}}$ is symmetric and the complex structure $\mathcal{J}$ is antisymmetric, $\mathcal{J}^{\mathrm{T}} = -\mathcal{J}$, it immediately follows that

$$\langle \Psi, \Phi\rangle_{\mathbb{C}} = \overline{\langle \Phi, \Psi\rangle_{\mathbb{C}}}. \tag{31}$$

Thus, the real space $\mathbb{R}^6$ endowed with the Euclidean metric and the operator $\mathcal{J}$ preserves the complete geometric and algebraic structure of $\mathbb{C}^3$. ■

2.3. Real Eigenmodes and Stueckelberg Orthogonality

To complete the formal propagating plane wave solution, we evaluate the null space of $\mathcal{M}$ to extract the eigenmodes for each branch of the dispersion relation. Let us define the magnitude of the horizontal wave vector as

$$k^2 \equiv k_x^2 + k_y^2. \tag{32}$$

Because we are operating in the reals, the arbitrary complex $U(1)$ phase is replaced by an $SO(2)$ kinematic rotational degeneracy between the cosine and sine quadratures. We fix this gauge by setting the height anomaly of the second quadrature to zero,

$$\eta_2 = 0. \tag{33}$$

For the stationary geostrophic branch, $\omega_0 = 0$, the relation $\mathcal{M}\Phi = 0$ yields a two-dimensional null space representing topological zero-modes. The first unnormalized state is then found to be,

$$\Phi_{G1} = \begin{pmatrix} 0 \\ 0 \\ f \\ k_y \\ -k_x \\ 0 \end{pmatrix}. \tag{34}$$

 doi:10.20944/preprints202605.0606.v2

Its orthogonal complement in the degenerate subspace is generated by applying the complex structure operator,

$$\Phi_{G2} = \mathcal{J}\Phi_{G1}. \tag{35}$$

Using the Euclidean inner product the squared norm of this state is

$$\langle \Phi_{G1}, \Phi_{G1} \rangle_{\mathbb{R}} = k^2 + f^2. \tag{36}$$

Because $\mathcal{J}$ is an orthogonal operator, $\mathcal{J}^{\mathrm{T}}\mathcal{J} = I_6$, it acts as an isometry, and thus Φ_{G2} possesses the identical norm. The fully normalized geostrophic mode pairs are therefore

$$\hat{\Phi}_{G1} = \frac{1}{\sqrt{k^2+f^2}} \begin{pmatrix} 0 \\ 0 \\ f \\ k_y \\ -k_x \\ 0 \end{pmatrix}, \quad \hat{\Phi}_{G2} = \frac{1}{\sqrt{k^2+f^2}} \begin{pmatrix} -k_y \\ k_x \\ 0 \\ 0 \\ 0 \\ f \end{pmatrix}. \tag{37}$$

For the propagating Poincaré waves, $\omega_{\pm} \neq 0$, we use the dispersion relation identity $k^2 = \omega^2 - f^2$. Solving $\mathcal{M}\Phi = 0$ yields the primary unnormalized vectors,

$$\Phi_{P1} = \begin{pmatrix} \omega k_x \\ \omega k_y \\ k^2 \\ -f k_y \\ f k_x \\ 0 \end{pmatrix}, \quad \Phi_{N1} = \begin{pmatrix} -\omega k_x \\ -\omega k_y \\ k^2 \\ -f k_y \\ f k_x \\ 0 \end{pmatrix}. \tag{38}$$

Taking the inner product of, say, Φ_{P1} with itself, we find

$$\langle \Phi_{P1}, \Phi_{P1} \rangle_{\mathbb{R}} = \omega^2 k^2 + k^4 + f^2 k^2 = k^2(\omega^2 + k^2 + f^2) = 2k^2\omega^2. \tag{39}$$

Defining the normalization factor, $\mathcal{N} = \sqrt{2}k\omega$, the normalized propagating positive-frequency eigenmodes are

$$\hat{\Phi}_{P1} = \frac{1}{\sqrt{2}k\omega} \begin{pmatrix} \omega k_x \\ \omega k_y \\ k^2 \\ -f k_y \\ f k_x \\ 0 \end{pmatrix}, \quad \hat{\Phi}_{P2} = \frac{1}{\sqrt{2}k\omega} \begin{pmatrix} f k_y \\ -f k_x \\ 0 \\ \omega k_x \\ \omega k_y \\ k^2 \end{pmatrix}, \tag{40}$$

where $\hat{\Phi}_{P2} = \mathcal{J}\hat{\Phi}_{P1}$. Similarly, the negative-frequency eigenmodes are

$$\hat{\Phi}_{N1} = \frac{1}{\sqrt{2}k\omega} \begin{pmatrix} -\omega k_x \\ -\omega k_y \\ k^2 \\ -f k_y \\ f k_x \\ 0 \end{pmatrix}, \quad \hat{\Phi}_{N2} = \frac{1}{\sqrt{2}k\omega} \begin{pmatrix} f k_y \\ -f k_x \\ 0 \\ -\omega k_x \\ -\omega k_y \\ k^2 \end{pmatrix}, \tag{41}$$

where $\hat{\Phi}_{N2} = \mathcal{J}\hat{\Phi}_{N1}$. Because the classical fluid system possesses a particle-hole-like symmetry, the geometric and topological properties of this latter negative branch are symmetric to those of the positive branch. Therefore, we restrict our subsequent geometric analysis to the positive-frequency modes

 doi:10.20944/preprints202605.0606.v2

and the geostrophic zero-modes. Together these are sufficient to fully characterize the topological invariants of the system while ensuring the mathematical completeness of the $\mathbb{R}^6$ basis.

Finally, a fundamental requirement of our basis is that these degenerate pairs must be orthogonal. We verify this by exploiting the inherent antisymmetric nature of $\mathcal{J}$. For any real normalized state $\hat{\Phi}$ and its Stueckelberg partner $\mathcal{J}\hat{\Phi}$, their Euclidean inner product is given by the quadratic form,

$$\langle \hat{\Phi}, \mathcal{J}\hat{\Phi} \rangle_{\mathbb{R}} = \hat{\Phi}^{\mathrm{T}} \mathcal{J} \hat{\Phi}. \tag{42}$$

Because $\mathcal{J}^{\mathrm{T}} = -\mathcal{J}$, the corresponding real quadratic form vanishes for all states. This guarantees that

$$\langle \hat{\Phi}_{G1}, \hat{\Phi}_{G2} \rangle_{\mathbb{R}} = 0, \quad \langle \hat{\Phi}_{P1}, \hat{\Phi}_{P2} \rangle_{\mathbb{R}} = 0, \quad \langle \hat{\Phi}_{N1}, \hat{\Phi}_{N2} \rangle_{\mathbb{R}} = 0, \tag{43}$$

securing an orthonormal basis for the real Hilbert space construction without relying on complex conjugation.

2.4. General Solution

With the complete set of normalized mutually orthogonal six-dimensional eigenmodes secured we can now map these states back to physical space to construct the general spatial-temporal solution, $\Psi(\boldsymbol{x}, t)$, for the original three-component planetary fluid system governed by Eq. (7).

Recall that the six-dimensional real state vector separates the harmonic quadratures, storing the cosine amplitudes in the upper three components and the sine amplitudes in the lower three components. We can formalize the return to the physical three-dimensional wave field by defining a 3×6 phase projection operator,

$$\mathcal{P}(\theta) = \begin{pmatrix} \cos\theta\, I_3 & \sin\theta\, I_3 \end{pmatrix}, \tag{44}$$

where I_3 is the 3×3 identity matrix, and θ is the standard kinematic phase argument. For any given dynamical branch $b \in \{G, P, N\}$, this phase angle is defined as

$$\theta_b(\boldsymbol{k}, \boldsymbol{x}, t) = \boldsymbol{k} \cdot \boldsymbol{x} - \omega_b(\boldsymbol{k}) t, \tag{45}$$

where the respective frequencies for each branch are the stationary geostrophic mode $\omega_0 = 0$, the positive Poincaré mode $\omega_+ = \sqrt{k^2 + f^2}$, and the negative Poincaré mode $\omega_- = -\sqrt{k^2 + f^2}$.

Because the Stueckelberg partners $\hat{\Phi}_{b1}(\boldsymbol{k})$ and $\hat{\Phi}_{b2}(\boldsymbol{k})$ span the complete orthogonal degenerate subspace for each branch at a specified wave vector $\boldsymbol{k}$, an arbitrary fluid excitation is simply a real linear combination of these two basis states. Integrating over all possible continuous wave vectors and summing over the three dynamical branches, the most general physical solution takes the form

$$\Psi(\boldsymbol{x}, t) = \int \frac{d^2k}{(2\pi)^2} \sum_{b \in \{G,P,N\}} \mathcal{P}(\theta_b) \Big[c_{b1}(\boldsymbol{k}) \hat{\Phi}_{b1}(\boldsymbol{k}) + c_{b2}(\boldsymbol{k}) \hat{\Phi}_{b2}(\boldsymbol{k}) \Big]. \tag{46}$$

Here, $c_{b1}(\boldsymbol{k})$ and $c_{b2}(\boldsymbol{k})$ are *real* scalar amplitude distributions, uniquely determined by the initial boundary conditions of the fluid system.

This continuous formulation highlights the mechanical elegance of the real Stueckelberg approach. By substituting the relation $\hat{\Phi}_{b2} = \mathcal{J}\hat{\Phi}_{b1}$ we can observe how the complex structure operator interacts with the spatial phase projector. If we partition the primary state into its upper and lower three-dimensional blocks as $\hat{\Phi}_{b1} = (\Psi_1, \Psi_2)^{\mathrm{T}}$, the action of $\mathcal{J}$ yields $(-\Psi_2, \Psi_1)^{\mathrm{T}}$. Applying the projector to this partnered state gives,

$$\mathcal{P}(\theta)\mathcal{J}\hat{\Phi}_{b1} = \begin{pmatrix} \cos\theta\, I_3 & \sin\theta\, I_3 \end{pmatrix} \begin{pmatrix} -\Psi_2 \\ \Psi_1 \end{pmatrix} = \sin\theta\, \Psi_1 - \cos\theta\, \Psi_2, \tag{47}$$

which is equivalent to applying a continuous $\pi/2$ phase shift to the original real-valued wave. Thus, linearly mixing the two real orthogonal states via the continuous scalar coefficients c_{b1} and c_{b2} replicates

 doi:10.20944/preprints202605.0606.v2

the rotational utility of an arbitrary complex amplitude $Ae^{i\phi}$. It reproduces the full spectrum of the fluid's kinematics entirely within the $\mathbb{R}^6$ domain, eliminating the necessity of introducing complex wave fields.

2.5. Comparison with the Complex Formalism

Before proceeding to the computation of the geometric tensor it is instructive to further compare the real Stueckelberg approach developed above with the standard three-dimensional complex formulation.

In the complex formulation the wave solutions to the physical equations of motion, Eq. (7), are constructed by employing a complex plane wave Ansatz,

$$\Psi_{\mathbb{C}}(\boldsymbol{x}, t) = \tilde{\Psi} e^{i(\boldsymbol{k}\cdot\boldsymbol{x} - \omega(\boldsymbol{k})t)}, \tag{48}$$

where $\tilde{\Psi} \in \mathbb{C}^3$ is a three-dimensional complex amplitude vector. Under this Ansatz, the real spatial differential operator

$$L_{\text{sp}} = F + D \tag{49}$$

transforms into the 3×3 complex matrix,

$$L_{\mathbb{C}} = F + iK. \tag{50}$$

The time evolution then requires

$$-i\omega(\boldsymbol{k})\tilde{\Psi} = (F + iK)\tilde{\Psi}, \tag{51}$$

which may be re-arranged into a standard Hermitian-like eigenvalue problem in $\mathbb{C}^3$.

Mathematically the complex three-dimensional eigenvalue problem and the real six-dimensional eigenvalue problem in Eq. (12) are isomorphic. By identifying the complex amplitude as

$$\tilde{\Psi} = \Psi_1 - i\Psi_2, \tag{52}$$

the operation $(F + iK)(\Psi_1 - i\Psi_2)$ naturally reproduces the block matrix dynamics of our $\mathcal{G}$ operator. The efficiency and elegance of the complex formulation make it a powerful computational tool for extracting topological fluid invariants. However, from a physical standpoint, applying the complex formulation to a macroscopic classical fluid introduces subtle interpretive challenges that the real formulation inherently obviates.

First, the complex state $\tilde{\Psi}$ is defined up to an arbitrary local phase $e^{i\chi}$, reflecting the fundamental $U(1)$ gauge symmetry of complex quantum mechanics. In a macroscopic fluid, however, an abstract complex phase has no direct physical meaning. The Stueckelberg formulation clarifies that this $U(1)$ gauge freedom is not an abstract unobservable; it is mathematically identical to the $SO(2)$ kinematic rotational symmetry between the real, observable cosine and sine spatial quadratures of the wave. The "gauge choice" in the real formulation simply corresponds to defining the spatial origin (a phase shift) of the wave coordinate system.

Second, the complex formulation relies on the standard Hermitian inner product on $\mathbb{C}^3$ to derive the Fubini-Study metric and the Berry curvature [10]. As demonstrated in Sec. 2.2, the Stueckelberg synthesis unpacks this complex inner product into two distinct real components: a symmetric Euclidean dot product and an antisymmetric form mediated by the complex structure operator $\mathcal{J}$. This separation physically reinterprets the quantum geometry. The symmetric part represents the classical mechanical energy (inertia) of the fluid wave, while the antisymmetric part represents the symplectic area of the classical phase space.

Consequently, the real geometry formulation confirms that the topological features of the fluid are not mathematical artifacts generated by embedding the system into a complex vector space. Rather, the quantum-like geometry is an intrinsic property of the classical Newtonian kinematics of the rotating shallow water model.

 doi:10.20944/preprints202605.0606.v2

3. The Real Quantum Geometric Tensor

To investigate the topological properties of the fluid system we examine how the physical eigenmodes vary across the parameter space. For a wave packet propagating in a fluid at a fixed latitude, the active parameter space is the two-dimensional momentum space, parameterized by the wavevector $\boldsymbol{k} = (k_x, k_y)$. However, to reveal the topological structure of the dispersion bands (specifically, the band gap closure at the origin), following [10], we extend the parameter space to the three-dimensional vector $\boldsymbol{p} = (k_x, k_y, f)$ by treating the Coriolis parameter f as a continuous control variable. We also define the corresponding parametric derivatives as $\partial_\mu \equiv \partial/\partial p_\mu$, where the indices span $\mu, \nu \in \{k_x, k_y, f\}$.

In standard complex formulations the geometric properties of an energy band are encoded in the Quantum Geometric Tensor (QGT), constructed using the complex inner product and the band projector $P_{\mathbb{C}} = |\psi\rangle\langle\psi|$. In our real Stueckelberg formulation, we construct an equivalent geometric tensor using exclusively the six-dimensional real state vectors and the real Euclidean inner product.

Consider a specific dispersion branch (geostrophic or propagating) spanned by the degenerate, orthonormal 6D state pair $\{\hat{\Phi}_1, \hat{\Phi}_2\}$, where $\hat{\Phi}_2 = \mathcal{J}\hat{\Phi}_1$. The orthogonal projector $P(\boldsymbol{p})$ onto this two-dimensional real subspace is

$$P(\boldsymbol{p}) = \hat{\Phi}_1\hat{\Phi}_1^{\mathrm{T}} + \hat{\Phi}_2\hat{\Phi}_2^{\mathrm{T}} = \hat{\Phi}_1\hat{\Phi}_1^{\mathrm{T}} + \mathcal{J}\hat{\Phi}_1\hat{\Phi}_1^{\mathrm{T}}\mathcal{J}^{\mathrm{T}}. \tag{53}$$

This projector is gauge-invariant; it depends only on the physical subspace and is invariant under any $SO(2)$ rotation between the quadratures $\hat{\Phi}_1$ and $\hat{\Phi}_2$. Using the Stueckelberg synthesis of the complex inner product (Sec. 2.2) we define the Real Quantum Geometric Tensor (RQGT), $\mathcal{T}_{\mu\nu}$, by taking the derivatives of the primary quadrature state $\hat{\Phi}_1$ and projecting out the components that remain within the band,

$$\mathcal{T}_{\mu\nu} = \langle \partial_\mu\hat{\Phi}_1, (I_6 - P)\partial_\nu\hat{\Phi}_1\rangle_{\mathbb{R}} - i\langle \partial_\mu\hat{\Phi}_1, \mathcal{J}(I_6 - P)\partial_\nu\hat{\Phi}_1\rangle_{\mathbb{R}}, \tag{54}$$

where I_6 is the 6×6 identity matrix. The imaginary unit i is retained formally as a bookkeeping device to separate the symmetric and antisymmetric real bilinear forms.

The real part of $\mathcal{T}_{\mu\nu}$ is symmetric under the exchange of indices $\mu \leftrightarrow \nu$. This defines the real formulation of the Fubini-Study metric, $g_{\mu\nu}$, which measures the invariant infinitesimal distance between fluid states in the extended parameter space,

$$g_{\mu\nu} = (\partial_\mu\hat{\Phi}_1)^{\mathrm{T}}(I_6 - P)(\partial_\nu\hat{\Phi}_1) = -\hat{\Phi}_1^{\mathrm{T}}(\partial_\mu\partial_\nu P)\hat{\Phi}_1. \tag{55}$$

Because $g_{\mu\nu}$ relies solely on the symmetric Euclidean inner product it quantifies the sensitivity of the fluid's kinetic and potential energy to variations in the wavevector and background rotation, excluding trivial kinematic rotations within the degenerate band.

The "imaginary" component of Eq. (54) captures the antisymmetric geometry, leading to the Berry phase and Berry curvature. Correspondingly, we define the real Berry connection, A_μ, which describes how the $SO(2)$ angle between the quadratures twists through parameter space. In complex quantum mechanics, this is

$$A_\mu^{\mathbb{C}} = i\langle\psi|\partial_\mu\psi\rangle. \tag{56}$$

Here, applying our Stueckelberg mapping, this is implemented by the complex structure operator $\mathcal{J}$,

$$A_\mu = \langle\hat{\Phi}_1, \mathcal{J}\partial_\mu\hat{\Phi}_1\rangle_{\mathbb{R}} = \hat{\Phi}_1^{\mathrm{T}}\mathcal{J}\partial_\mu\hat{\Phi}_1. \tag{57}$$

To verify that A_μ acts as a proper gauge connection, consider a local $SO(2)$ gauge transformation rotating the state by an arbitrary parameter-dependent angle $\alpha(\boldsymbol{p})$,

$$\hat{\Phi}_1' = \cos\alpha\,\hat{\Phi}_1 + \sin\alpha\,\hat{\Phi}_2 = \cos\alpha\,\hat{\Phi}_1 + \sin\alpha\,\mathcal{J}\hat{\Phi}_1. \tag{58}$$

 doi:10.20944/preprints202605.0606.v2

Substituting $\hat{\Phi}_1'$ into Eq. (57), and using the relations $\mathcal{J}^2 = -I_6$, $\mathcal{J}^{\mathrm{T}} = -\mathcal{J}$, and the normalization $\hat{\Phi}_1^{\mathrm{T}}\hat{\Phi}_1 = 1$, we find

$$A_\mu' = A_\mu - \partial_\mu \alpha. \tag{59}$$

This confirms that A_μ transforms exactly as a $U(1)$ Abelian gauge field derived purely from classical fluid kinematics.

The gauge-invariant Berry curvature, $\Omega_{\mu\nu}$, is defined as the curl of the Berry connection,

$$\Omega_{\mu\nu} = \partial_\mu A_\nu - \partial_\nu A_\mu. \tag{60}$$

Substituting Eq. (57) yields

$$\Omega_{\mu\nu} = \partial_\mu(\hat{\Phi}_1^{\mathrm{T}}\mathcal{J}\partial_\nu\hat{\Phi}_1) - \partial_\nu(\hat{\Phi}_1^{\mathrm{T}}\mathcal{J}\partial_\mu\hat{\Phi}_1). \tag{61}$$

Applying the product rule the terms containing second derivatives $\partial_\mu\partial_\nu\hat{\Phi}_1$ commute and cancel. We are left with

$$\Omega_{\mu\nu} = (\partial_\mu\hat{\Phi}_1)^{\mathrm{T}}\mathcal{J}(\partial_\nu\hat{\Phi}_1) - (\partial_\nu\hat{\Phi}_1)^{\mathrm{T}}\mathcal{J}(\partial_\mu\hat{\Phi}_1) = (\partial_\mu\hat{\Phi}_1)^{\mathrm{T}}\mathcal{J}(\partial_\nu\hat{\Phi}_1) - (\mathcal{J}\partial_\mu\hat{\Phi}_1)^{\mathrm{T}}\partial_\nu\hat{\Phi}_1. \tag{62}$$

Because $\mathcal{J}^{\mathrm{T}} = -\mathcal{J}$, the second term becomes $(\partial_\mu\hat{\Phi}_1)^{\mathrm{T}}\mathcal{J}(\partial_\nu\hat{\Phi}_1)$, reducing the real Berry curvature to

$$\Omega_{\mu\nu} = 2(\partial_\mu\hat{\Phi}_1)^{\mathrm{T}}\mathcal{J}(\partial_\nu\hat{\Phi}_1). \tag{63}$$

Returning to the antisymmetric part of the RQGT in Eq. (54) we evaluate the term containing the projector P,

$$(\partial_\mu\hat{\Phi}_1)^{\mathrm{T}}\mathcal{J}P(\partial_\nu\hat{\Phi}_1) = (\partial_\mu\hat{\Phi}_1)^{\mathrm{T}}\left(\hat{\Phi}_2\hat{\Phi}_1^{\mathrm{T}} - \hat{\Phi}_1\hat{\Phi}_2^{\mathrm{T}}\right)(\partial_\nu\hat{\Phi}_1). \tag{64}$$

Because $\hat{\Phi}_1$ is normalized, its derivative is orthogonal to itself,

$$\hat{\Phi}_1^{\mathrm{T}}\partial_\nu\hat{\Phi}_1 = 0. \tag{65}$$

Consequently, both terms vanish. The projector P drops out of the antisymmetric component, leaving

$$\langle\partial_\mu\hat{\Phi}_1, \mathcal{J}(I_6 - P)\partial_\nu\hat{\Phi}_1\rangle_{\mathbb{R}} = (\partial_\mu\hat{\Phi}_1)^{\mathrm{T}}\mathcal{J}(\partial_\nu\hat{\Phi}_1) = \frac{1}{2}\Omega_{\mu\nu}. \tag{66}$$

Thus, the RQGT is compactly expressed as

$$\mathcal{T}_{\mu\nu} = g_{\mu\nu} - \frac{i}{2}\Omega_{\mu\nu}. \tag{67}$$

This confirms that the Fubini-Study metric and the Berry curvature emerge directly from the real 6D Euclidean geometry of the rotating shallow water equations, driven entirely by the antisymmetric kinematic matrix $\mathcal{J}$.

4. Explicit Matrix and Metric form of the Fubini-Study Metric

We now explicitly calculate the Fubini-Study metric $g_{\mu\nu}$ for the propagating Poincaré modes in the extended three-dimensional parameter space, $\boldsymbol{p} = (k_x, k_y, f)$. The invariant line element is given by the quadratic form,

$$ds^2 = g_{\mu\nu}dp^\mu dp^\nu. \tag{68}$$

 doi:10.20944/preprints202605.0606.v2

To construct the explicit 3×3 metric tensor we recall the primary normalized state vector for the positive-frequency Poincaré branch, $\omega_+ = \omega = \sqrt{k^2 + f^2}$,

$$\hat{\Phi}_{P1}(\boldsymbol{p}) = \frac{1}{\sqrt{2k\omega}} \begin{pmatrix} \omega k_x \\ \omega k_y \\ k^2 \\ -f k_y \\ f k_x \\ 0 \end{pmatrix}. \tag{69}$$

The Fubini-Study metric is defined as $g_{\mu\nu} = (\partial_\mu \hat{\Phi}_{P1})^{\mathrm{T}}(I_6 - P)(\partial_\nu \hat{\Phi}_{P1})$. Because the projector $P(\boldsymbol{p}) = \hat{\Phi}_{P1}\hat{\Phi}_{P1}^{\mathrm{T}} + \hat{\Phi}_{P2}\hat{\Phi}_{P2}^{\mathrm{T}}$ removes variations that merely rotate the state within the degenerate $SO(2)$ subspace, $g_{\mu\nu}$ isolates the gauge-invariant changes in the physical state. Applying the chain rule with respect to (k_x, k_y, f) and projecting the derivatives through $(I_6 - P)$ yields a real symmetric matrix. After algebraic simplification the explicit metric tensor defining the Riemannian geometry on the momentum-rotation parameter space is found to be

$$g_{\mu\nu} = \frac{1}{(k^2 + f^2)^2} \begin{pmatrix} k_y^2 + f^2 & -k_x k_y & -f k_x \\ -k_x k_y & k_x^2 + f^2 & -f k_y \\ -f k_x & -f k_y & k^2 \end{pmatrix}. \tag{70}$$

5. Explicit Antisymmetric 2-Form for the Berry Curvature

The symplectic component of the parameter space is governed by the real Berry curvature. As shown in Sec. 3 the curvature is defined by the antisymmetric 2-form,

$$\Omega_{\mu\nu} = 2(\partial_\mu \hat{\Phi}_{P1})^{\mathrm{T}} \mathcal{J} (\partial_\nu \hat{\Phi}_{P1}), \tag{71}$$

which translates into an alternating differential form in the three-dimensional space $\boldsymbol{p}$. This form maps to a pseudo-vector field $\boldsymbol{\Omega} = (\Omega_{k_y f}, \Omega_{f k_x}, \Omega_{k_x k_y})$ via the Levi-Civita symbol,

$$\Omega_\lambda = \frac{1}{2} \epsilon_{\mu\nu\lambda} \Omega_{\mu\nu}. \tag{72}$$

Evaluating this requires the inner product of the parametric derivatives of the primary state with its Stueckelberg partner, $\hat{\Phi}_{P2} = \mathcal{J}\hat{\Phi}_{P1}$, resulting in

$$\Omega_{\mu\nu} = 2 \left(\frac{\partial \hat{\Phi}_{P1}}{\partial p^\mu} \right)^{\mathrm{T}} \frac{\partial \hat{\Phi}_{P2}}{\partial p^\nu}. \tag{73}$$

Explicit calculation yields the antisymmetric curvature matrix,

$$\Omega_{\mu\nu} = \frac{1}{(k^2 + f^2)^{3/2}} \begin{pmatrix} 0 & -f & k_y \\ f & 0 & -k_x \\ -k_y & k_x & 0 \end{pmatrix}. \tag{74}$$

Here, the in-plane momentum component, $\Omega_{k_x k_y} = -f/\omega^3$, represents the accumulation of the classical phase as a wave packet is transported around a closed loop in the (k_x, k_y) momentum space

 doi:10.20944/preprints202605.0606.v2

at a fixed latitude f. Assembling these components, the total real Berry curvature 2-form is expressed as a dual vector field,[2]

$$\boldsymbol{\Omega}(\boldsymbol{p}) = \frac{C\boldsymbol{p}}{2|\boldsymbol{p}|^3}. \tag{75}$$

The antisymmetric geometry of the real Stueckelberg state vectors yields an exact topological magnetic monopole situated at the origin of the parameter space, $(k_x = 0, k_y = 0, f = 0)$. Unlike complex formulations where monopoles arise from the abstract geometry of Hermitian matrices, here the monopole emerges purely from the classical kinematic rotation matrix $\mathcal{J}$.

The topological charge of this monopole is exactly $C = -2$. The absolute value $|C| = 2$ corresponds to the number of topologically protected edge states (Kelvin and Yanai modes) that must bridge the topological gaps between the distinct bulk bands when the physical fluid domain is bounded.[3] The negative sign encodes the eastward chirality of this spectral flow, a result which aligns with our calculation of the Witten index of $W = -2$ in Sec. 8 below. This demonstrates an exact structural consistency of our mathematical approach: the topological invariant of the high-frequency propagating bands, C, mirrors the invariant of the unbroken zero-energy geostrophic vacuum, W.

6. Scale Invariance and the Null Subspace of the Metric

As noted by Ganeshan and Dorsey [10], the 3×3 Fubini-Study metric tensor possesses a one-dimensional null subspace. This null subspace reflects the scale invariance of the classical fluid equations.

The normalized primary state vector $\hat{\Phi}_{P1}$ is a homogeneous function of degree zero with respect to the parameters. Specifically, the numerator of each component carries a combined polynomial degree of 2 in the variables (k_x, k_y, f), which is exactly balanced by the denominator $k\omega$. Consequently, scaling the parameter vector by an arbitrary positive constant λ, such that $(k_x, k_y, f) \to (\lambda k_x, \lambda k_y, \lambda f)$, scales the fluid frequency linearly as $\omega \to \lambda\omega$, but leaves the state vector $\hat{\Phi}_{P1}$ unchanged. Moving radially outward from the origin in the parameter space increases the energy of the wave but preserves the relative amplitudes and phase differences of the fluid mode. Because the physical state does not vary along this radial direction, the directional derivative of the state projected along the radial parameter vector $\boldsymbol{p} = (k_x, k_y, f)^{\mathrm{T}}$ must vanish,

$$p^\mu \partial_\mu \hat{\Phi}_{P1} = k_x \frac{\partial \hat{\Phi}_{P1}}{\partial k_x} + k_y \frac{\partial \hat{\Phi}_{P1}}{\partial k_y} + f \frac{\partial \hat{\Phi}_{P1}}{\partial f} = 0. \tag{76}$$

Contracting the metric tensor with this radial vector yields zero,

$$g_{\mu\nu} p^\nu = 0. \tag{77}$$

Thus, the vector $\boldsymbol{p}$ spans the one-dimensional null subspace of the metric.

---

[2] The factor of 2 in the denominator is the standard normalization for a topological monopole in a three-dimensional parameter space. The Chern number is formally defined as $C = (1/2\pi) \oint \boldsymbol{\Omega} \cdot d\boldsymbol{S}$. Integrating the general monopole formula $\boldsymbol{\Omega}(\boldsymbol{p}) = C\boldsymbol{p}/(2|\boldsymbol{p}|^3)$ over a closed spherical manifold using the outward surface element $d\boldsymbol{S} = \hat{\boldsymbol{p}}|\boldsymbol{p}|^2 d\Omega_{\text{solid}}$ yields $(C/2) \oint d\Omega_{\text{solid}} = (C/2)(4\pi) = 2\pi C$, which correctly normalizes the invariant. Equating this geometric definition to our explicitly derived fluid curvature pseudo-vector, $\boldsymbol{\Omega}(\boldsymbol{p}) = -\boldsymbol{p}/|\boldsymbol{p}|^3$, determines the integer topological charge to be $C = -2$.

[3] Note that in topological band theory, there is the corresponding concept of "spectral flow" which refers to the continuous transfer of states from one topological bulk band to another across a spectral gap as a parameter (like momentum k_x) varies. In the rotating shallow water system, the "gap" is not just a single empty void from $-f$ to $+f$. There are actually three distinct bulk sectors: the upper Poincaré band, with $\omega \geq |f|$, the flat geostrophic/Rossby band, with $\omega \approx 0$, and the lower Poincar'e band, with $\omega \leq -|f|$ (refer to Fig. A1 in Appendix A). For the system to satisfy the bulk-boundary correspondence with $|C| = 2$, there must be two distinct branches that connect these isolated bulk bands. The Kelvin wave traverses the entire region, crossing $\omega = 0$ to connect the negative Poincaré band to the positive Poincaré band. The Yanai wave (mixed Rossby-gravity wave) acts as the second bridge: as $k_x \to -\infty$, its frequency asymptotes toward the low-frequency Rossby band, $\omega \to 0$; as $k_x \to +\infty$, it merges with the high-frequency Poincaré band. Therefore, the Yanai wave "flows" across the gap that separates the zero-energy bulk sector from the high-energy bulk sector. The fact that it bridges topologically distinct bulk bands without crossing $\omega = 0$ is still a direct manifestation of the topological spectral flow mandated by $|C| = 2$.

 doi:10.20944/preprints202605.0606.v2

To explicitly isolate this null subspace we perform a coordinate transformation from the Cartesian parameters (k_x, k_y, f) to spherical parameters (p, θ, ϕ), where the radial coordinate is defined directly by the wave frequency,

$$p = \sqrt{k_x^2 + k_y^2 + f^2} = \omega. \tag{78}$$

In this spherical basis the radial geometric variations are governed by the partial derivative $\partial/\partial p$. Because the state vectors are independent of the radial magnitude p, all p-derivatives vanish. Consequently, in the spherical parameter basis, the transformed Fubini-Study metric $\tilde{g}_{ab}$ assumes a block-diagonal form with an explicit zero on the diagonal (cf. [10]),

$$\tilde{g}_{ab} = \begin{pmatrix} 0 & 0 & 0 \\ 0 & g_{\theta\theta} & g_{\theta\phi} \\ 0 & g_{\phi\theta} & g_{\phi\phi} \end{pmatrix}. \tag{79}$$

This demonstrates that all invariant geometric variations of the fluid modes reside exclusively on the two-dimensional surface of the parameter sphere parameterized by the angles θ and ϕ. The radial dimension acts as a null gauge direction, confirming that the topological monopole charge is entirely determined by the angular winding of the real fluid state.

7. Planetary Evolution and Experimental Geometric Parameter Sweep

In condensed matter systems the control parameters of a topological Hamiltonian can be tuned explicitly via external magnetic fields or strain. In our real rotating fluid formulation the background rotation f acts as the analogous macroscopic control parameter. While we cannot physically alter the rotation rate of the modern Earth to experimentally verify the geometric sensitivities encoded in our Fubini-Study metric, the geological history of the planet has naturally performed this parameter sweep over deep time.

During the Archean eon, approximately three to four billion years ago, the Earth rotated significantly faster, with a day lasting approximately 14 hours. The global Coriolis parameter f was correspondingly larger. To understand the geometric consequence of this regime we rely on the fundamental length scale of rotating shallow water theory, the Rossby radius of deformation, L_R,

$$L_R = \frac{\sqrt{gH}}{f}, \tag{80}$$

where g is gravity and H is the equivalent fluid depth.

The Rossby radius characterizes the spatial extent of rotationally trapped fluid structures, including topologically protected boundary modes such as equatorial Kelvin waves. Because L_R is inversely proportional to f the primordial Earth possessed a significantly smaller Rossby radius. The energy gap separating the low-frequency geostrophic modes from the high-frequency propagating Poincaré modes, which is proportional to f at the origin of momentum space, was wider.

Planetary weather systems and ocean eddies in this high-f regime would have been tightly confined, creating narrow zonal jets. The topologically protected edge modes would have been compressed against boundaries. Over billions of years tidal friction generated by the moon has steadily decreased f. This gradual tidal braking has swept the Earth's oceans and atmosphere through a continuous adiabatic geometric evolution, lowering the band gap, expanding the Rossby radius, and shifting the fluid modes through the geometric curvatures described by our real Fubini-Study metric.

While the fossil record does not preserve high-frequency fluid dynamics, the rigorous scaling laws of our real geometric formulation guarantee that this planetary evolution can be replicated at the laboratory scale. We propose a macroscopic geophysical fluid dynamics (GFD) laboratory experiment designed to physically execute this parameter sweep and explicitly measure the geometric tensors derived in Secs. 4 and 5.

 doi:10.20944/preprints202605.0606.v2

The experimental setup consists of a parabolic rotating tank filled with a shallow layer of fluid, mounted on a motorized turntable. To ensure the fluid dynamics remain in the linear rotationally-dominated regime required by the Stueckelberg Hamiltonian the experimental fluid parameters must satisfy a small Rossby number, $Ro \ll 1$, and a small Ekman number $Ek \ll 1$.

To replicate the conditions of the Archean oceans the tank is initially spun up to a high angular velocity $\Omega_{\max}$, establishing a wide band gap. A wavemaker positioned at the radial boundary continuously injects a broad spectrum of wave energy into the system. Particle image velocimetry (PIV) captures the real high-resolution Eulerian velocity field $\boldsymbol{u}(x, y, t)$ and the free surface elevation $\eta(x, y, t)$. This provides direct empirical access to the physical six-dimensional real Stueckelberg state vectors $\hat{\Phi}$ at every point in the basin. The experimental procedure operates as follows:

1. **Steady state Initialization:** The system is driven at high f. The PIV measurements verify the tight spatial confinement of the boundary modes and the wide spectral gap between the geostrophic eddies and the bulk Poincaré waves.
2. **The parameter sweep:** The turntable is decelerated, acting as an artificial tidal brake. This sweeps the control parameter f downward toward the modern Earth regime, and ultimately toward $f = 0$ (the exact topological degeneracy point where the band gap closes).
3. **Extracting the geometry:** During the spin-down the real-time PIV data is Fourier-transformed to track the evolution of the fluid eigenmodes in momentum space. By measuring the changing inner products of the physical state vectors as f decreases we directly compute the real parametric derivatives $\partial_f \hat{\Phi}$.

This approach allows for the empirical reconstruction of the g_{ff} and cross-term $g_{k_x f}$ components of the Fubini-Study metric. As $f \to 0$, the experiment directly captures the closing of the energy gap, the macroscopic spatial widening of the boundary modes, and the divergent geometric sensitivity predicted by the metric. By mapping real fluid variables to real geometric tensors this table-top analog would physically validate the Stueckelberg parameter space geometry without relying on complex abstract spaces.

8. Unbroken Supersymmetry in the Real Stueckelberg Formulation

An interesting consequence of mapping the classical rotating shallow water equations into the real Stueckelberg Hilbert space is that the system naturally admits an exact unbroken supersymmetric interpretation. Rather than standard global supersymmetric quantum mechanics, the kinematics of the classical fluid induce a momentum-dependent graded (Clifford) structure, acting as a supersymmetric algebra over a continuous parameter space bundle.

In Witten's formulation the defining characteristic of a supersymmetric system is the existence of a self-adjoint supercharge operator, $\mathcal{Q}$, from which the system's non-negative energy Hamiltonian, $\mathcal{H}_{\text{SUSY}}$, is generated via its square,

$$\mathcal{H}_{\text{SUSY}} = \mathcal{Q}^2. \tag{81}$$

Within our real six-dimensional approach the symmetric Stueckelberg Hamiltonian derived in Sec. 2.2 fulfills the role of the fundamental supercharge. We explicitly define this real symmetric supercharge matrix as

$$\mathcal{Q} \equiv \mathcal{H}_S = \begin{pmatrix} -K & F \\ -F & -K \end{pmatrix} = \begin{pmatrix} 0 & 0 & k_x & 0 & f & 0 \\ 0 & 0 & k_y & -f & 0 & 0 \\ k_x & k_y & 0 & 0 & 0 & 0 \\ 0 & -f & 0 & 0 & 0 & k_x \\ f & 0 & 0 & 0 & 0 & k_y \\ 0 & 0 & 0 & k_x & k_y & 0 \end{pmatrix}. \tag{82}$$

 doi:10.20944/preprints202605.0606.v2

Because the supercharge $\mathcal{Q}$ is a purely real and symmetric operator its square is guaranteed to generate a positive semi-definite real symmetric matrix. We therefore define the true supersymmetric Hamiltonian of the fluid by squaring the supercharge,

$$\mathcal{H}_{\text{SUSY}} = \mathcal{Q}^2 = \begin{pmatrix} k_x^2 + f^2 & k_x k_y & 0 & 0 & 0 & f k_y \\ k_x k_y & k_y^2 + f^2 & 0 & 0 & 0 & -f k_x \\ 0 & 0 & k^2 & -f k_y & f k_x & 0 \\ 0 & 0 & -f k_y & k_x^2 + f^2 & k_x k_y & 0 \\ 0 & 0 & f k_x & k_x k_y & k_y^2 + f^2 & 0 \\ f k_y & -f k_x & 0 & 0 & 0 & k^2 \end{pmatrix}. \tag{83}$$

By acting with this supersymmetric operator on our Stueckelberg basis states we obtain the eigenvalue equation,

$$\mathcal{H}_{\text{SUSY}} \Phi = \omega^2 \Phi. \tag{84}$$

The eigenvalues of this Hamiltonian are the squared frequencies of the physical fluid waves, perfectly aligning with the non-negative energy spectrum required by the algebra of supersymmetry,

$$E = \omega^2 \geq 0. \tag{85}$$

The physical importance of this identification lies in the classification of the fluid's topological spectrum. In supersymmetric theory a supersymmetry is considered "unbroken" if and only if there exists a ground state vacuum, $|0\rangle$, that is annihilated by the supercharge, resulting in zero energy,

$$\mathcal{Q}|0\rangle = 0 \implies E = 0. \tag{86}$$

For our planetary fluid system we apply the real supercharge to the geostrophic zero-modes derived in Sec. 2.3, giving

$$\mathcal{Q}\hat{\Phi}_{G1} = 0, \quad \text{and} \quad \mathcal{Q}\hat{\Phi}_{G2} = 0. \tag{87}$$

This reveals a physically interesting correspondence: the classical steady-state geostrophic balance—the fundamental mechanism driving large-scale weather patterns and ocean currents on Earth—is mathematically identical to the unbroken supersymmetric vacuum of the parameter space. The topological zero-modes of the fluid are precisely the unbroken supersymmetric ground states.

Furthermore, the standard supersymmetric algebra demands that all excited states with $E > 0$ must consist of degenerate multiplet pairs, formally identified as even-graded and odd-graded superpartners, which transform into one another under the action of the supercharge. In our fluid system these excited states correspond to the propagating gravity waves (the Poincaré modes), which possess strictly positive supersymmetric energy, $E = \omega^2 = k^2 + f^2 > 0$. Because the supercharge operator intrinsically couples the scalar height anomalies to the horizontal velocities through spatial gradients, a propagating gravity wave is a hybridized state consisting of both potential energy and kinetic energy sectors, naturally satisfying the superpartner requirements of Witten's algebra.

Separately, the system also possesses a twofold kinematic degeneracy guaranteed by the antisymmetric complex structure operator $\mathcal{J}$. Because the generator of the dynamics commutes with $\mathcal{J}$, our supercharge also commutes with the complex structure,

$$[\mathcal{Q}, \mathcal{J}] = 0. \tag{88}$$

Consequently, if $\hat{\Phi}_{P1}$ is a propagating eigenmode of $\mathcal{Q}$, its Stueckelberg partner $\hat{\Phi}_{P2} = \mathcal{J}\hat{\Phi}_{P1}$ is guaranteed to be an orthogonal eigenstate with the identical eigenvalue. This simply reflects the $SO(2)$ rotational gauge freedom between the sine and cosine quadratures of the physical wave.

To complete the supersymmetric classification of our fluid system we must establish a mathematical mechanism to distinguish between the superpartners. In standard SUSY QM this is achieved by

 doi:10.20944/preprints202605.0606.v2

defining a chiral grading operator, commonly denoted as Γ (the direct analog of the parity operator $(-1)^F$ or the Dirac γ_5 matrix). This operator partitions the Hilbert space into two distinct sectors: an "even-graded" sector with eigenvalue $+1$, and an "odd-graded" sector with eigenvalue -1. For the supersymmetry to be exact, the grading operator must anti-commute with the supercharge, $\{\Gamma, \mathcal{Q}\} = 0$.

In our formulation the underlying hydrodynamic description of shallow water provides a very intuitive and physically meaningful *momentum-dependent* grading operator that formally partitions the fluid velocity field into its Helmholtz decomposed components, divergence and vorticity. Our construction proceeds as follows:

Let $k^2 = k_x^2 + k_y^2$, and define the unit wave vector,

$$\hat{\boldsymbol{k}} = \boldsymbol{k}/k = (k_x, k_y)^{\mathrm{T}}/k. \tag{89}$$

We introduce the geometric reflection operator across the momentum vector as

$$\gamma_{2\times 2} = 2\hat{\boldsymbol{k}}\hat{\boldsymbol{k}}^{\mathrm{T}} - I_2 = \begin{pmatrix} c & s \\ s & -c \end{pmatrix}, \tag{90}$$

where

$$c = (k_x^2 - k_y^2)/k^2, \quad s = 2k_x k_y/k^2 \tag{91}$$

are the geometric ratios satisfying

$$c^2 + s^2 = 1. \tag{92}$$

Operating within the 6×6 real Hilbert space defined by the basis $(u_1, v_1, \eta_1, u_2, v_2, \eta_2)^{\mathrm{T}}$, we now define the real symmetric involutory, $\Gamma^2 = I_6$, chiral grading matrix as

$$\Gamma = \begin{pmatrix} c & s & 0 & 0 & 0 & 0 \\ s & -c & 0 & 0 & 0 & 0 \\ 0 & 0 & -1 & 0 & 0 & 0 \\ 0 & 0 & 0 & c & s & 0 \\ 0 & 0 & 0 & s & -c & 0 \\ 0 & 0 & 0 & 0 & 0 & -1 \end{pmatrix}. \tag{93}$$

To understand the physical significance of this grading let us examine the eigenspace[4] of its 2×2 velocity sub-blocks. Because $c^2 + s^2 = 1$, the eigenvalues of $\gamma_{2\times 2}$ are $+1$ and -1, such that:

1. The eigenvector corresponding to the $+1$ eigenvalue is proportional to $\boldsymbol{k} = (k_x, k_y)^{\mathrm{T}}$. In fluid mechanics, this corresponds to the longitudinal, or *divergent*, velocity component of the flow, $\nabla \cdot \mathbf{u} \neq 0$. We formally designate this purely divergent velocity space as the even-graded (*"bosonic"*) sector.
2. The eigenvector corresponding to the -1 eigenvalue is proportional to $(-k_y, k_x)^{\mathrm{T}}$. This represents the transverse, or *rotational*, velocity component of the flow, which carries the fluid's vorticity, $\nabla \times \mathbf{u} \neq 0$. Furthermore, the scalar height anomaly η is assigned an eigenvalue of -1 by the matrix in Eq. (93). We formally designate the combined rotational velocity and scalar height fields as the odd-graded (*"fermionic"*) sector.

It is important to notice that the geometric ratios c and s diverge at $k = 0$, meaning that the chiral grading operator $\Gamma(\boldsymbol{k})$ is undefined at the origin. Physically, this reflects the impossibility of

[4] This eigenspace projection is the momentum-space realization of the Helmholtz decomposition. In real space the Helmholtz theorem separates a continuous vector field into an irrotational (curl-free) and a solenoidal (divergence-free) component. In Fourier space the spatial derivative ∇ transforms into the algebraic multiplier $i\boldsymbol{k}$. Consequently, the decomposition algebraically projects the velocity field into a longitudinal component parallel to the wave vector $\boldsymbol{k} = (k_x, k_y)^{\mathrm{T}}$ (representing the flow divergence) and a transverse component orthogonal to $\boldsymbol{k}$ (representing the flow vorticity). The chiral grading operator Γ thereby mathematically partitions the fluid into its irreducible Helmholtz components, assigning the divergent kinetic energy to the even-graded sector and the rotational kinetic energy to the odd-graded sector.

 doi:10.20944/preprints202605.0606.v2

performing a Helmholtz decomposition on a spatially uniform field. Geometrically, this is not merely a coordinate singularity; it is the exact topological obstruction underlying the Berry monopole described in previous sections. The mathematical impossibility of defining a smooth, global longitudinal-transverse decomposition over the entire momentum space constitutes a nontrivial chiral bundle. The singular momentum-space Dirac grading and the emergent Berry topology are dual manifestations of the same fundamental geometric obstruction.

Away from the origin, this specific momentum-dependent grading operator preserves the exact chiral symmetry of the algebra, *even in the presence of planetary rotation*, when $f \neq 0$. By carrying out the block matrix multiplication it can be straightforwardly shown that the spatial gradients contained within the kinematic blocks of $\mathcal{Q}$ are absorbed by the ratios c and s, yielding an exact anti-commutation. Simultaneously, the velocity sub-blocks of Γ anti-commute with the antisymmetric Coriolis blocks of $\mathcal{Q}$. Therefore, for all values of f, the exact chiral symmetry algebra holds true,

$$\{\Gamma, \mathcal{Q}\} = \Gamma\mathcal{Q} + \mathcal{Q}\Gamma = 0, \quad [\Gamma, \mathcal{H}_{\text{SUSY}}] = 0, \quad \mathcal{H}_{\text{SUSY}} = \mathcal{Q}^2. \tag{94}$$

The anti-commutation relation guarantees that for every state Φ with energy E, the superpartner state $\Gamma\Phi$ has energy $-E$. Because $\mathcal{H}_{\text{SUSY}} = \mathcal{Q}^2$ gives the physical energy squared, this enforces that all non-zero energy modes (the propagating Poincaré waves) must exist in symmetric pairs.

The ultimate utility of this exact chiral grading lies in the calculation of the Witten Index, W, a topological invariant that counts the difference between the number of even-graded, n_B, and odd-graded, n_F, zero-energy ground states. Because our grading operator depends on momentum, this evaluation is technically a local fiberwise index. At fixed momentum $\boldsymbol{k} \neq 0$, the local supersymmetric index is formally defined as the trace of the grading operator over the entire Hilbert space,

$$W = \text{Tr}(\Gamma) = n_B - n_F. \tag{95}$$

Taking the trace of our explicit 6×6 grading matrix in Eq. (93) requires summing the diagonal elements. The trace of the upper velocity block is $c + (-c) = 0$, and the trace of the lower velocity block is likewise 0. The two scalar height components each contribute -1. Thus, the sum evaluates to

$$W = -2. \tag{96}$$

This simple integer result is physically important. A fundamental theorem of supersymmetric quantum mechanics states that if $W \neq 0$, the supersymmetry cannot be dynamically broken (see Appendix B for more detail). The non-vanishing topological index formally guarantees the existence of at least $|W|$ mutually orthogonal zero-energy ground states.

In our fluid system $|W| = 2$ guarantees the existence of exactly two unbroken zero-modes. Because the geostrophic states obey geostrophic balance, their velocity fields are purely rotational (divergence-free). Consequently, they possess no even-graded (divergent) components, $n_B = 0$, and populate entirely within the odd-graded (vorticity and height) sector, $n_F = 2$, yielding the local index $W = 0 - 2 = -2$.

Thus, we arrive at the following topological conclusion: at any valid momentum, the permanent existence of large-scale, steady-state geostrophic weather patterns on a rotating planet is topologically protected by the non-zero local fiberwise Witten index of the classical fluid's real kinematics.

It is instructive to contrast this supersymmetric classification with the foundational topological characterization introduced by Delplace *et al.* [3]. In their complexified approach the topological invariants of the fluid are identified by calculating the Chern numbers of the energy bands. This process requires integrating the Berry curvature over the entire parameter space manifold to predict the emergence of propagating high-frequency edge modes (the Kelvin and Yanai waves) via the bulk-boundary correspondence.

 doi:10.20944/preprints202605.0606.v2

In contrast, our derivation of the index $W = -2$ is arrived at purely algebraically from the exact chiral grading of the real physical variables, bypassing the need for global integration over a complexified fiber bundle. While the Chern number characterizes the global geometric twisting of the excited dynamically propagating waves, the real local Witten index acts as a spectral invariant that directly counts the unbroken zero-energy geostrophic modes. Together, these two distinct topological invariants provide a complementary picture of planetary fluids: the Chern number topologically protects the propagating edge states, whereas our real fiberwise index provides the topological protection ensuring the permanent existence of the slow steady-state geostrophic bulk patterns.

9. Explicit Construction of the Superpartner States

The exact chiral symmetry established by the momentum-dependent grading operator Γ allows us to explicitly construct the even-graded and odd-graded superpartners of the fluid system. Using the standard projection operators of supersymmetric quantum mechanics,

$$\mathcal{P}_B = \frac{I_6 + \Gamma}{2}, \qquad \mathcal{P}_F = \frac{I_6 - \Gamma}{2}, \tag{97}$$

we can decompose the physical fluid eigenmodes derived in Sec. 2.3 into their purely even-graded ($+1$ eigenvalue) and purely odd-graded (-1 eigenvalue) components.

Let us first examine the excited supersymmetric states with $E > 0$, which correspond to the propagating Poincaré gravity waves. Applying the projection operators to the first physical quadrature state, $\hat{\Phi}_{P1}$, we isolate its underlying superpartners. The normalized even-graded (divergent) superpartner is found in the upper Stueckelberg block,

$$\hat{\Phi}_{B1} = \frac{1}{k} \begin{pmatrix} k_x \\ k_y \\ 0 \\ 0 \\ 0 \\ 0 \end{pmatrix}. \tag{98}$$

The corresponding normalized odd-graded (vortical) superpartner contains the hybridized rotational velocity and scalar height fields,

$$\hat{\Phi}_{F1} = \frac{1}{k\omega} \begin{pmatrix} 0 \\ 0 \\ k^2 \\ -fk_y \\ fk_x \\ 0 \end{pmatrix}. \tag{99}$$

It is straightforward to verify that these two pure states satisfy the supersymmetric algebra, transforming into one another under the action of the real supercharge,

$$\mathcal{Q}\hat{\Phi}_{B1} = \omega\hat{\Phi}_{F1}, \quad \text{and} \quad \mathcal{Q}\hat{\Phi}_{F1} = \omega\hat{\Phi}_{B1}. \tag{100}$$

These two superpartners together reconstruct the physical gravity wave; the propagating Poincaré mode is an equal superposition of its respective even and odd components,

$$\hat{\Phi}_{P1} = \frac{1}{\sqrt{2}}(\hat{\Phi}_{B1} + \hat{\Phi}_{F1}). \tag{101}$$

 doi:10.20944/preprints202605.0606.v2

By the geometric rotational symmetry of the system applying the projectors to the second physical quadrature state, $\hat{\Phi}_{P2}$, extracts the orthogonal superpartner doublet. The even-graded superpartner resides in the lower Stueckelberg block,

$$\hat{\Phi}_{B2} = \frac{1}{k}\begin{pmatrix} 0 \\ 0 \\ 0 \\ k_x \\ k_y \\ 0 \end{pmatrix}, \tag{102}$$

while its corresponding odd-graded superpartner is

$$\hat{\Phi}_{F2} = \frac{1}{k\omega}\begin{pmatrix} fk_y \\ -fk_x \\ 0 \\ 0 \\ 0 \\ k^2 \end{pmatrix}. \tag{103}$$

Just as before, these states satisfy

$$\mathcal{Q}\hat{\Phi}_{B2} = \omega\hat{\Phi}_{F2}, \quad \mathcal{Q}\hat{\Phi}_{F2} = \omega\hat{\Phi}_{B2}, \tag{104}$$

and the physical wave is their exact superposition,

$$\hat{\Phi}_{P2} = \frac{1}{\sqrt{2}}(\hat{\Phi}_{B2} + \hat{\Phi}_{F2}). \tag{105}$$

Thus, the propagating gravity waves furnish representations of the supersymmetric pairing structure induced by the real Stueckelberg algebra.

We now turn our attention to the unbroken supersymmetric vacuum with $E = 0$. First, notice that the geostrophic states are entirely devoid of any divergent velocity components, and that the transverse velocity fields $(-k_y, k_x)$ are eigenvectors of the velocity sub-blocks with an eigenvalue of -1. Therefore, applying the chiral grading operator Γ to the geostrophic modes gives

$$\Gamma\hat{\Phi}_{G1} = -\hat{\Phi}_{G1}, \quad \Gamma\hat{\Phi}_{G2} = -\hat{\Phi}_{G2}. \tag{106}$$

Correspondingly, the even-graded projection of the geostrophic modes is zero,

$$\mathcal{P}_B\hat{\Phi}_G = 0, \tag{107}$$

while the odd-graded projection returns the states unaltered,

$$\mathcal{P}_F\hat{\Phi}_G = \hat{\Phi}_G. \tag{108}$$

This provides the explicit proof for our Witten index calculation. The classical geostrophic zero-modes are exclusively and entirely odd-graded. Because there are no even-graded ground states, $n_B = 0$, and two orthogonal odd-graded ground states, $n_F = 2$, the topological index evaluating to $W = -2$ is now verified by the explicit eigenstates of the fluid system.

 doi:10.20944/preprints202605.0606.v2

10. Resolution of the Real Wave and Mode Selection Ambiguities

While the topological origin of equatorial waves was established by Delplace *et al.* [3], the reliance on a complexified pseudo-spin mapping left conceptual ambiguities. These were highlighted by Biello and Dimofte [11], who raised two concerns regarding the application of quantum topological methods to classical fluids. First, they noted that quantum winding numbers arise from the rotating phase of complex-valued wave functions; if classical physical waves are real-valued linear combinations of these complex states, it must be explained why the topological winding numbers do not cancel through destructive interference. Second, they pointed out that quantum electron systems rely on a Fermi sea at zero temperature to determine the ground state, fixing the chirality of edge states. Because classical fluids lack a Pauli exclusion principle or a Fermi sea, arbitrary pairings of bulk modes across the equator could theoretically predict both eastward and westward equatorial modes. A topological theory must provide a mechanism that governs the observed eastward propagation of Kelvin waves.

The real Stueckelberg six-dimensional formalism, combined with the momentum-dependent chiral algebraic structure, resolves both ambiguities.

Regarding the first concern (the cancellation of real topological winding), the derivation demonstrates that the Berry curvature in classical fluids is not an artifact of a complex quantum phase. By separating the complex quantum geometric tensor into its real Fubini-Study metric $g_{\mu\nu}$ and its real Berry curvature $\Omega_{\mu\nu}$, we showed that the curvature is a symplectic geometric form. The rotational phase is generated by the real antisymmetric complex structure operator $\mathcal{J}$, which enforces an $SO(2)$ kinematic rotation between the orthogonal sine and cosine quadratures of the wave. Because the macroscopic states $\hat{\Phi}_1$ and $\hat{\Phi}_2 = \mathcal{J}\hat{\Phi}_1$ act as independent orthogonal basis vectors in $\mathbb{R}^6$, their wedge products do not cancel upon superposition. Together, they define a real oriented area in the parameter space. The topological monopole charge of $C = -2$ is therefore an invariant property of the fluid's real symplectic kinematics, independent of a complex phase.

Regarding the second concern (the lack of a Fermi sea for mode selection), the mapping to the momentum-dependent graded (Clifford) algebra provides the classical selection mechanism. In this continuous supersymmetric framework, the effective spectrum is defined by $E = \omega^2 = k^2 + f^2$. This yields degenerate positive-energy superpartners containing both the forward-propagating Poincaré modes (the P branch, $\omega > 0$) and the reverse-propagating modes (the N branch, $\omega < 0$).

The fluid is governed by an isolated zero-energy vacuum sector with $E = 0$, topologically protected by the local fiberwise index $W = -2$. Because the Berry monopole charge $C = -2$ and the local chiral index $W = -2$ are dual manifestations of the identical geometric Helmholtz obstruction at the $k = 0$ origin, this continuous algebraic isolation naturally replaces the role of the quantum Fermi sea. In fluid dynamics, these odd-graded zero-energy modes correspond to the conservation of potential vorticity (PV). Because the geostrophic vacuum is algebraically isolated from the propagating bands by the Coriolis parameter f, the bulk-boundary correspondence is strictly constrained.

When f changes sign across the planetary equator the spectral flow must bridge the gap between the excited Poincaré bands and the $W = -2$ vacuum. While the forward (P) and reverse (N) propagating bulk modes share the same squared supersymmetric energy E, they belong to orthogonal sectors defined by their physical frequency ω. Time-reversal symmetry is broken by the planetary rotation f. Consequently, integrating the real Berry curvature over the positive-frequency sub-manifold yields the exact monopole charge $C = -2$, specifying the spectral winding direction. Because the fluid must connect the positive-frequency bulk band to the zero-energy PV vacuum as $f \to -f$, the strict mathematical symmetry between the propagating band topology $C = -2$ and the local vacuum invariant $W = -2$ selects edge modes with a strictly positive group velocity. The arbitrary pairing of northern and southern bulk states is algebraically prohibited by the isolation of the fiberwise index, guaranteeing the eastward propagation of equatorial Kelvin waves without invoking a quantum Fermi sea.

 doi:10.20944/preprints202605.0606.v2

11. Conclusion

In this paper, we demonstrated that the topological phenomena inherent to planetary fluid dynamics do not require explicit complex coordinate representation or abstract Hamiltonians. By mapping the classical rotating shallow water equations into a real, six-dimensional Stueckelberg Hilbert space, we showed that the topological band structure of planetary waves is an intrinsic property of the fluid's kinematics in $\mathbb{R}^6$.

Through this purely real formulation we decoupled the conventional complex quantum geometric tensor into its fundamental geometric constituents. We established that the Fubini-Study metric and the Berry curvature act as independent, real geometric objects. This approach explicitly revealed the emergence of a topological magnetic monopole of charge $C = -2$ arising purely from the real antisymmetric rotational kinematics of the classical wave quadratures. By retaining the state vectors in the physical basis of fluid variables the real Fubini-Study metric explicitly captured the scale invariance of the fluid via a one-dimensional null subspace and accurately reflected the coordinate singularities mathematically analogous to the Dirac string.

To physically ground these geometric properties we connected the parameter space structure to macroscopic geophysical phenomena. By leveraging the dynamic similarity governed by the Rossby radius of deformation we treated the continuous variation of the Coriolis parameter f as a model for the adiabatic geometric evolution of the Archean Earth. We translated this planetary-scale parameter sweep into an experimental proposal utilizing rotating laboratory tanks, providing a tabletop mechanism to directly measure the real parametric derivatives and geometric tensors as the fluid approaches the topological degeneracy point at $f = 0$.

Finally, we established an exact mathematical equivalence between the rotating shallow water equations and a momentum-dependent graded Clifford structure. By identifying the symmetric Stueckelberg Hamiltonian as a purely real supercharge, we showed that the classical fluid realizes an exact chiral algebraic structure over a momentum bundle. Through the explicit geometric construction of a momentum-dependent chiral grading operator based on the Helmholtz decomposition, we calculated a local fiberwise Witten index of $W = -2$. This discrete spectral invariant algebraically counts the two odd-graded zero-energy geostrophic modes, proving that the permanent existence of large-scale weather patterns is a topologically protected consequence of this continuous chiral algebra. Because the Berry monopole charge $C = -2$ and the local chiral index $W = -2$ are dual manifestations of the identical singular Helmholtz obstruction at the momentum origin their fundamental mathematical symmetry provides the exact geometric selection mechanism for the eastward propagation of equatorial boundary waves, resolving the classical mode selection ambiguity without the need for a quantum Fermi sea.

Ultimately, this real geometric and chiral algebraic formulation provides a mathematically rigorous framework for analyzing classical topological systems. It demonstrates that the foundational principles of topological band theory and supersymmetric algebras are not exclusive to complex quantum mechanics, but are intrinsically woven into the macroscopic geometry and kinematics of planetary fluids.

Appendix A The Geophysical Waves and Their Topological Origins

This Appendix re-derives the physical waves present in the rotating shallow water model on the basis of the Stueckelberg formalism. It also explains how these waves fit into the broader story of topological physics discussed in this paper.

To understand how topology applies to oceans and atmospheres, it is helpful to look at the fluid in two distinct regions: the open ocean (the bulk) and the equator (the boundary).

Appendix A.1 The Bulk: The Open Ocean and the Frequency Gap

When analyzing a localized region of the ocean far from the equator, the Earth's rotation provides a roughly constant Coriolis parameter, f. In the equations of motion, this rotation acts similarly to

 doi:10.20944/preprints202605.0606.v2

a mass term in the Dirac equation. It breaks time-reversal symmetry and creates a frequency gap between different types of fluid motion.

In this bulk region, we find two primary categories of flow:

1. **Poincaré Waves (Inertio-Gravity Waves):** These are relatively high-frequency gravity waves, much like the ripples created by dropping a stone into a pond, but their trajectories are curved by the planet's rotation. They have a dispersion relation of $\omega_{\pm}(\boldsymbol{k}) = \pm\omega$, where $\omega = \sqrt{k^2 + f^2}$. In our 6d formalism, this wave has the form,

$$\hat{\Phi}_{P1}(\boldsymbol{k}) = \frac{1}{\sqrt{2k\omega}} \begin{pmatrix} \omega k_x \\ \omega k_y \\ k^2 \\ -f k_y \\ f k_x \\ 0 \end{pmatrix}, \tag{A109}$$

which encapsulates both the velocity components and the height anomaly, preserving the orthogonal rotational quadratures in the lower block. In the language of topological band theory, these waves form the excited energy bands of the fluid. The geometric properties of these specific waves, such as their Berry curvature and topological monopole charge, are the primary subjects of recent quantum geometric studies, including the recent work by Ganeshan and Dorsey [10], as well as the derivations in the main text of this paper.

2. **Geostrophic Zero-Modes:** These are the slow, large-scale, stationary flow patterns, such as major ocean currents or atmospheric jet streams. They sit at a frequency of $\omega_0(\boldsymbol{k}) = 0$ and are characterized by the conservation of potential vorticity. In our 6d formalism, this wave has the form,

$$\hat{\Phi}_{G1}(\boldsymbol{k}) = \frac{1}{\sqrt{k^2 + f^2}} \begin{pmatrix} 0 \\ 0 \\ f \\ k_y \\ -k_x \\ 0 \end{pmatrix}, \tag{A110}$$

which demonstrates that these stationary modes possess zero divergence and correspond to the geostrophic balance condition. In the supersymmetric formulation discussed in this manuscript, these steady flows serve as the stable ground state, or vacuum, of the system.

Appendix A.2 The Boundary: The Equator as a Domain Wall

Because the Earth is a sphere, the Coriolis parameter f is not uniform. It is largest at the poles, approaches zero at the equator, and changes sign between the Northern and Southern Hemispheres. A common approximation near the equator is

$$f \approx \beta y, \tag{A111}$$

where y is the North-South coordinate. This Coriolis parameter breaks translational symmetry in the North-South direction. We no longer have a plane wave in y; we only have a 1D plane wave traveling in x, so the physical 3D wave takes the form,

$$\Psi(x, y, t) = \Psi_1(y, k_x)\cos(k_x x - \omega t) + \Psi_2(y, k_x)\sin(k_x x - \omega t). \tag{A112}$$

Because y now defines the shape of the bound spatial profile rather than a Fourier momentum variable, those y-dependent profiles act as the amplitudes for the 1D wave. When we stack these quadratures

 doi:10.20944/preprints202605.0606.v2

into our Stueckelberg formalism, the 6D state $\Psi(y, k_x) = (\Psi_1^{\mathrm{T}}, \Psi_2^{\mathrm{T}})^{\mathrm{T}}$ naturally retains a y-dependence, becoming the position-dependent amplitude vector in the 6D representation.

In topological physics, when a mass-like parameter such as f changes sign across a spatial line, that line acts as a domain wall. A core principle called the bulk-boundary correspondence states that if the bulk waves (the Poincaré waves) possess a non-trivial topological structure, gapless edge states must emerge along the domain wall. These edge states are required to bridge the frequency gap between the high-frequency bulk bands and the zero-frequency ground state.

Appendix A.3 The Equatorial Waves: Matsuno's Solutions

Long before topological band theory was formulated, Taroh Matsuno [6] (1966) solved the shallow water equations near the equator and cataloged the waves that are naturally trapped there. Because the equator traps these waves, their amplitude decays as one moves further North or South. Three prominent equatorial waves emerged from his analysis (see Fig. A1):

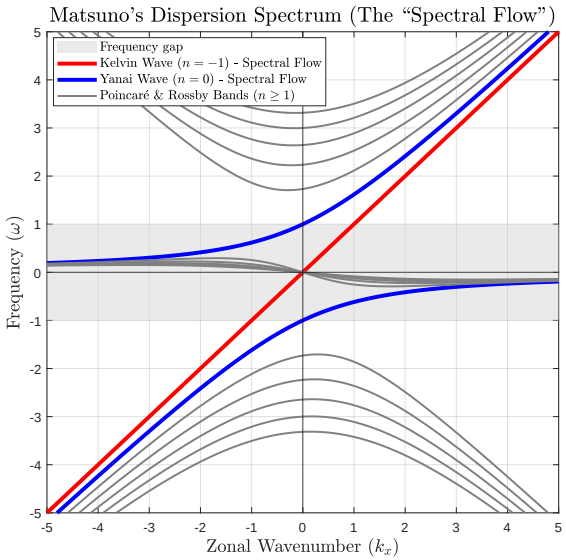

Figure A1. Matsuno's dispersion spectrum illustrating the topological spectral flow of equatorial waves (here $\beta = 1$). The gray contours represent the standard bulk modes ($n \geq 1$), which separate into high-frequency Poincaré gravity waves and low-frequency Rossby waves. The light gray region denotes the forbidden frequency gap where bulk modes cannot exist. As required by the low-frequency limit, $-k_x/\omega \approx 2n + 1 + k_x^2$, of the dispersion relation, Eq. (A138), the Rossby bands for $\omega > 0$ occupy the negative k_x domain, enforcing their westward propagation. The Kelvin ($n = -1$, red) and Yanai ($n = 0$, blue) modes exhibit continuous spectral flow, acting as boundary states that bridge the frequency gap and connect the isolated bulk bands across the momentum space.

1. **The Equatorial Kelvin Wave:** This is a boundary wave that travels parallel to the equator with no North-South fluid velocity. It travels only in the eastward direction, and its frequency is proportional to its wavenumber, $\omega = k_x$. With a spatial envelope bounded by the equator,

$$E_0(y) = e^{-\beta y^2/2}, \tag{A113}$$

and an eastward dispersion,

$$\omega = k_x, \tag{A114}$$

 doi:10.20944/preprints202605.0606.v2

the 6d quadrature state for this wave takes the form,

$$\Phi_{\text{Kelvin}}(y, k_x) = E_0(y) \begin{pmatrix} 1 \\ 0 \\ 1 \\ 0 \\ 0 \\ 0 \end{pmatrix}. \tag{A115}$$

This sparse vector explicitly visualizes how the Kelvin wave possesses zero meridional velocity, $v = 0$, and maintains perfectly synchronized zonal velocity and height anomalies, $u = \eta$. Topologically, this wave acts as a chiral edge state that connects the geostrophic zero-modes to the high-frequency Poincaré bands.

2. **The Yanai Wave (Mixed Rossby-Gravity Wave):** This wave exhibits hybrid behavior. At high frequencies, it acts like an eastward-moving gravity wave, while at low frequencies, it acts like a westward-moving Rossby wave. Like the Kelvin wave, it also helps bridge the frequency gap. Representing a mixed hybrid state, the Yanai wave combines the lowest-order Gaussian envelope $E_0(y)$ with the first-order Hermite polynomial spatial mode,

$$E_1(y) \propto y e^{-\beta y^2/2}. \tag{A116}$$

The 6d quadrature state for this wave takes the form,

$$\Phi_{\text{Yanai}}(y, k_x) \propto \begin{pmatrix} u_{\text{Yanai}}(y) \\ 0 \\ \eta_{\text{Yanai}}(y) \\ 0 \\ v_{\text{Yanai}}(y) \\ 0 \end{pmatrix} \propto \begin{pmatrix} \omega E_1(y) \\ 0 \\ \omega E_1(y) \\ 0 \\ E_0(y) \\ 0 \end{pmatrix} \propto \begin{pmatrix} E_1(y) \\ 0 \\ E_1(y) \\ 0 \\ (\omega - k_x) E_0(y) \\ 0 \end{pmatrix}, \tag{A117}$$

where we used the fact that for $n = 0$, $\omega(\omega - k_x) = \beta$ (see Eq. (A138)). The cross-band coupling of this mixed mode is evident in the frequency-dependent amplitudes, allowing it to interpolate between gravity-like and Rossby-like behavior.

3. **Equatorial Rossby Waves:** These are low-frequency waves that propagate westward and are driven primarily by the spatial variation of the Coriolis parameter β. Governed by higher-order Hermite polynomials $E_n(y)$, with $n \geq 1$, due to the spatial variation of the Coriolis force, the purely westward propagating equatorial Rossby waves are characterized by strong rotational vorticity. The 6d quadrature state for this wave takes the form,

$$\Phi^{(n)}_{\text{Rossby}}(y, k_x) = \begin{pmatrix} u_n(y) \\ 0 \\ \eta_n(y) \\ 0 \\ v_n(y) \\ 0 \end{pmatrix}, \tag{A118}$$

where $v_n(y) \propto E_n(y)$, and the zonal velocity $u_n(y)$ and height anomaly $\eta_n(y)$ are combinations of $E_{n-1}(y)$ and $E_{n+1}(y)$. In this real 6d representation, the topological properties make their spectral flow occupy the negative k_x domain. In other words, the underlying geometry of the rotating planet guarantees that these Rossby waves must exist, and it mathematically forces them to only ever travel westward.

 doi:10.20944/preprints202605.0606.v2

Appendix A.4 Deriving Matsuno's Spatial Envelopes via Real Quadratures

The standard derivation of the equatorial waves relies on substituting a complex wave Ansatz into the shallow water equations. Here we re-derive the spatial envelopes $E_n(y)$ within the real Hilbert space framework.

We begin with the linearized shallow water equations on the equatorial beta-plane, where the Coriolis parameter is expanded as $f = \beta y$,

$$\begin{aligned} \partial_t u - \beta y v + \partial_x \eta &= 0, && \text{(A119)} \\ \partial_t v + \beta y u + \partial_y \eta &= 0, && \text{(A120)} \\ \partial_t \eta + \partial_x u + \partial_y v &= 0. && \text{(A121)} \end{aligned}$$

Instead of a complex phase, we project the physical 3d wave field onto two orthogonal harmonic quadratures. By exploiting the $SO(2)$ Stueckelberg gauge symmetry established in Section 2.3, we lock the zonal velocity and height anomaly into the cosine quadrature, and assign the meridional velocity to the sine quadrature. The real continuous wave field is then defined as

$$\begin{aligned} u(x,y,t) &= U(y)\cos(k_x x - \omega t), && \text{(A122)} \\ v(x,y,t) &= V(y)\sin(k_x x - \omega t), && \text{(A123)} \\ \eta(x,y,t) &= H(y)\cos(k_x x - \omega t). && \text{(A124)} \end{aligned}$$

Here, the spatial profiles $U(y)$, $V(y)$, and $H(y)$ act as the position-dependent amplitude states for our 6d vector $\Phi(y, k_x)$. Substituting this real ansatz into the fluid equations and dividing out the harmonic terms yields a coupled system of purely real ordinary differential equations,

$$\begin{aligned} \omega U - \beta y V - k_x H &= 0, && \text{(A125)} \\ -\omega V + \beta y U + \partial_y H &= 0, && \text{(A126)} \\ \omega H - k_x U + \partial_y V &= 0. && \text{(A127)} \end{aligned}$$

Appendix A.4.1 The Kelvin wave envelope

The equatorial Kelvin wave is defined by the absence of North-South flow, setting $V(y) = 0$ everywhere. Substituting this boundary condition into Eq. (A125) and (A127) requires that $\omega U = k_x H$ and $\omega H = k_x U$. This enforces a strictly non-dispersive, eastward-propagating solution where $\omega = k_x$ and $U(y) = H(y)$. Substituting $V = 0$ and $U = H$ into the remaining Eq. (A126) gives,

$$\beta y H + \partial_y H = 0 \implies \frac{\partial H}{\partial y} = -\beta y H. \quad \text{(A128)}$$

Integrating this first-order separable equation generates the fundamental Gaussian decay envelope,

$$H(y) \propto e^{-\frac{\beta y^2}{2}} \equiv E_0(y). \quad \text{(A129)}$$

Appendix A.4.2 The Kelvin wave envelope

The equatorial Kelvin wave is defined by the absence of North-South flow, setting $V(y) = 0$ everywhere. Substituting this boundary condition into Eq. (A125) and (A127) requires that $\omega U = k_x H$ and $\omega H = k_x U$. Together, these relations lead to $\omega^2 = k_x^2$, which algebraically admits two possible dispersion branches: $\omega = k_x$, with $U = H$, and $\omega = -k_x$, with $U = -H$. To determine which of these branches represents a physically realizable state, we substitute both candidate solutions into the remaining meridional momentum balance, Eq. (A126).

 doi:10.20944/preprints202605.0606.v2

For the $\omega = k_x$ branch where $U = H$, Eq. (A126) becomes

$$\beta y H + \partial_y H = 0 \implies \frac{\partial H}{\partial y} = -\beta y H. \tag{A130}$$

Integrating this first-order separable equation generates a Gaussian decay envelope,

$$H(y) \propto e^{-\frac{\beta y^2}{2}} \equiv E_0(y). \tag{A131}$$

This spatial profile naturally decays as $y \to \pm\infty$, representing a normalizable bound state that is correctly trapped along the equator.

Conversely, testing the westward-propagating branch, $\omega = -k_x$, with $U = -H$, in Eq. (A126) gives

$$-\beta y H + \partial_y H = 0 \implies \frac{\partial H}{\partial y} = \beta y H, \tag{A132}$$

and thus,

$$H(y) \propto e^{+\beta y^2/2}. \tag{A133}$$

Because this envelope grows exponentially toward infinity at high latitudes it produces an unnormalizable unphysical wavefunction and must be discarded. Therefore, the spatial boundary conditions of the fluid reject the westward solution, isolating the eastward-propagating $\omega = k_x$ mode as the unique equatorial Kelvin wave.

Appendix A.4.3 The higher-order envelopes and the harmonic oscillator

For the Yanai, Poincaré, and Rossby waves, the meridional velocity is non-zero, $V \neq 0$. To find the spatial profiles for these waves, we eliminate $U(y)$ and $H(y)$ to isolate $V(y)$.

Multiplying Eq. (A125) by ω and Eq. (A127) by k_x, then taking their sum, yields an expression for $U(y)$,

$$U(y) = \frac{1}{\omega^2 - k_x^2}\left(\omega\beta y V - k_x \partial_y V\right). \tag{A134}$$

Similarly, multiplying Eq. (A125) by k_x and Eq. (A127) by ω gives $H(y)$,

$$H(y) = \frac{1}{\omega^2 - k_x^2}\left(k_x\beta y V - \omega \partial_y V\right). \tag{A135}$$

We then substitute Eqs. (A134) and (A135) into Eq. (A126),

$$-\omega V + \frac{\beta y}{\omega^2 - k_x^2}\left(\omega\beta y V - k_x \partial_y V\right) + \frac{1}{\omega^2 - k_x^2}\partial_y\left(k_x\beta y V - \omega \partial_y V\right) = 0. \tag{A136}$$

Expanding the derivative in the final term, $\partial_y(k_x\beta y V) = k_x\beta V + k_x\beta y \partial_y V$, cancels the first-order derivatives of V. Multiplying the entire equation by $-(\omega^2 - k_x^2)/\omega$ leaves a single second-order differential equation,

$$\frac{d^2V}{dy^2} + \left[\left(\omega^2 - k_x^2 - \frac{k_x\beta}{\omega}\right) - \beta^2 y^2\right] V = 0. \tag{A137}$$

This is equivalent to the 1d Schrödinger equation for a quantum harmonic oscillator. For the fluid anomalies to remain physically bounded at high latitudes, $y \to \pm\infty$, the constant term inside the brackets must equal an odd integer multiple of β,

$$\omega^2 - k_x^2 - \frac{k_x\beta}{\omega} = \beta(2n+1), \quad n = 0, 1, 2, \dots . \tag{A138}$$

This boundary requirement naturally quantizes the dispersion relation for the Yanai ($n = 0$) and Rossby/Poincaré ($n \geq 1$) bands. Because this is the harmonic oscillator equation, its bound eigenstates

 doi:10.20944/preprints202605.0606.v2

are the Hermite polynomials $H_n(\sqrt{\beta}y)$ modulated by the ground-state Gaussian. Thus, the 6d quadrature states spontaneously organize into the quantized spatial envelopes,

$$E_n(y) = H_n(\sqrt{\beta}y)e^{-\frac{\beta y^2}{2}}. \tag{A139}$$

Appendix A.5 The topological literature

With the basic waves defined, we can trace how physicists have recently connected these classical fluid phenomena to topological quantum mechanics.

1. The topological connection (2017): Delplace, Marston, and Venaille [3] recognized that Matsuno's fluid equations could be mapped onto the Hamiltonian of a topological insulator. They calculated the Chern numbers of the bulk Poincaré bands and applied the bulk-boundary correspondence. This analysis showed that the Kelvin and Yanai waves are not just mathematical solutions, but are topologically guaranteed to exist due to the geometric twisting of the bulk Poincaré waves.

2. The physical questions (2017): In the accompanying perspective, Biello and Dimofte [11] raised two important physical questions about applying quantum topology to classical fluids. First, quantum winding numbers rely on the rotating phase of complex-valued wave functions, but physical fluid waves are inherently real. If we combine complex waves to form real ones, it was unclear why the topological winding numbers would not simply cancel out. Second, quantum electron systems have a Fermi sea (a filled ground state up to a certain energy) that enforces the direction in which edge states must travel. Fluids lack a Fermi sea, leading to the question of what specific mechanism forces the Kelvin wave to travel eastward rather than allowing westward boundary modes.

3. Quantum geometry in fluids (2026): More recently, Ganeshan and Dorsey [10] investigated the detailed quantum geometry of the bulk Poincaré waves, explicitly deriving the complex quantum geometric tensor. Their work clarified the geometric structure of the bulk bands, though it relied on a complex mapping that left the question of real-valued classical waves open.

4. The real and supersymmetric resolution proposal: Finally, this paper addresses the remaining open questions. By reformulating the fluid in a fully real, six-dimensional Stueckelberg parameter space, we find that the Berry curvature is a real symplectic geometric feature, not an artifact of a complex phase. This explains how real classical waves retain their topological winding without cancellation. Furthermore, by showing that the fluid equations share the mathematical structure of supersymmetric quantum mechanics, we identify the geostrophic zero-modes as an unbroken vacuum state. This vacuum mathematically replaces the quantum Fermi sea, restricting the system's spectral flow and guaranteeing that the boundary modes (Kelvin waves) must travel eastward to bridge the gap between the vacuum and the excited bulk bands.

Appendix B Proof of Witten's theorem in the finite-dimensional real parameter space

In infinite-dimensional quantum field theories proving the topological invariance of the Witten index requires careful handling of states escaping to infinity or non-normalizable boundary conditions. In the real Stueckelberg formulation of the rotating shallow water model at a fixed wave vector the parameter space is a finite-dimensional real vector space, $\mathbb{R}^6$. In this finite-dimensional regime Witten's theorem is a direct mathematical consequence of the real spectral theorem of linear algebra.

Below we explicitly prove that the Witten index $W = \mathrm{Tr}(\Gamma)$ counts the difference between the number of bosonic and fermionic zero-energy vacuum states in a real Hilbert space, guaranteeing their topological protection.

Definitions

We define the real, finite-dimensional supersymmetric algebra of our fluid system. Utilizing the momentum-dependent grading operator introduced in Sec. 8, this chiral algebra holds for all values of the Coriolis parameter f,

 doi:10.20944/preprints202605.0606.v2

1. **The grading operator (Γ):** A real, symmetric involution matrix,

$$\Gamma^{\mathrm{T}} = \Gamma, \quad \Gamma^2 = I_6. \tag{A140}$$

It partitions the $\mathbb{R}^6$ space into a bosonic sector (eigenvalue $+1$) and a fermionic sector (eigenvalue -1).

2. **The supercharge ($\mathcal{Q}$):** A real, symmetric matrix,

$$\mathcal{Q}^{\mathrm{T}} = \mathcal{Q}. \tag{A141}$$

3. **Exact chiral symmetry:** The supercharge anticommutes with the grading operator,

$$\{\Gamma, \mathcal{Q}\} = \Gamma\mathcal{Q} + \mathcal{Q}\Gamma = 0 \implies \Gamma\mathcal{Q} = -\mathcal{Q}\Gamma. \tag{A142}$$

4. **The Hamiltonian ($\mathcal{H}$):** The energy operator is generated directly by the square of the supercharge,

$$\mathcal{H} \equiv \mathcal{Q}^2. \tag{A143}$$

Step 1: Positive semi-definite energy

Let Φ be an arbitrary real state vector in $\mathbb{R}^6$. The expected energy of this state is given by the inner product,

$$E = \Phi^{\mathrm{T}}\mathcal{H}\Phi = \Phi^{\mathrm{T}}\mathcal{Q}^2\Phi. \tag{A144}$$

Because the supercharge is a real symmetric matrix, $\mathcal{Q}^{\mathrm{T}} = \mathcal{Q}$, we may rewrite this as

$$E = \Phi^{\mathrm{T}}\mathcal{Q}^{\mathrm{T}}\mathcal{Q}\Phi = (\mathcal{Q}\Phi)^{\mathrm{T}}(\mathcal{Q}\Phi) = ||\mathcal{Q}\Phi||^2. \tag{A145}$$

Because the dot product of any real vector with itself is non-negative it follows that $E \geq 0$. In addition, $E = 0$ if and only if $\mathcal{Q}\Phi = 0$, meaning that any zero-energy states are annihilated by the supercharge.

Step 2: Commutation and simultaneous eigenstates

We examine the commutation relation between the grading operator and the energy Hamiltonian,

$$\Gamma\mathcal{H} = \Gamma(\mathcal{Q}\mathcal{Q}) = (\Gamma\mathcal{Q})\mathcal{Q} = (-\mathcal{Q}\Gamma)\mathcal{Q} = -\mathcal{Q}(\Gamma\mathcal{Q}) = -\mathcal{Q}(-\mathcal{Q}\Gamma) = \mathcal{Q}^2\Gamma = \mathcal{H}\Gamma. \tag{A146}$$

Because $\Gamma\mathcal{H} = \mathcal{H}\Gamma$, the operators commute, $[\Gamma, \mathcal{H}] = 0$.

By the real spectral theorem, any set of mutually commuting real symmetric matrices can be simultaneously diagonalized. This guarantees the existence of a complete orthonormal basis of six vectors for $\mathbb{R}^6$, where every basis vector Φ_i is a simultaneous eigenstate of both energy, E_i, and parity, ± 1.

Step 3: Pairing of the strictly positive energy states

Assume there exists a bosonic state Φ_B with strictly positive energy $E > 0$. By definition, $\mathcal{H}\Phi_B = E\Phi_B$ and $\Gamma\Phi_B = (+1)\Phi_B$.

We apply the supercharge to generate a transformed state, $\Psi = \mathcal{Q}\Phi_B$, and evaluate its properties:

1. **Fermionic parity:** $\Gamma\Psi = \Gamma(\mathcal{Q}\Phi_B) = -\mathcal{Q}(\Gamma\Phi_B) = -\mathcal{Q}(+1\Phi_B) = -\mathcal{Q}\Phi_B = -1\Psi$. The transformed state is a fermion.
2. **Energy preservation:** $\mathcal{H}\Psi = \mathcal{Q}^2(\mathcal{Q}\Phi_B) = \mathcal{Q}(\mathcal{Q}^2\Phi_B) = \mathcal{Q}(E\Phi_B) = E(\mathcal{Q}\Phi_B) = E\Psi$. The transformed state shares the exact same energy E.
3. **Non-triviality:** $||\Psi||^2 = \Psi^{\mathrm{T}}\Psi = (\mathcal{Q}\Phi_B)^{\mathrm{T}}(\mathcal{Q}\Phi_B) = \Phi_B^{\mathrm{T}}\mathcal{H}\Phi_B = E||\Phi_B||^2$. Because $E > 0$ and Φ_B is not the zero vector, $||\Psi||^2 > 0$, confirming the state exists.

 doi:10.20944/preprints202605.0606.v2

This establishes a strict bijection. For every individual bosonic state with $E > 0$, there exists an exact, linearly independent fermionic state with the identical energy. Therefore, all $E > 0$ states in the finite-dimensional space must exist in degenerate boson-fermion pairs.

Step 4: Topological protection of the Witten index

The Witten index is defined as the trace of the grading matrix,

$$W = \mathrm{Tr}(\Gamma). \tag{A147}$$

Because the trace is invariant under basis transformations, we evaluate it in our simultaneous eigenbasis. The trace is the sum of the Γ eigenvalues for all six basis states,

$$W = \sum_{i=1}^{6} \langle \Phi_i | \Gamma | \Phi_i \rangle. \tag{A148}$$

We partition this sum into states with strictly positive energy and states with zero energy,

$$W = \sum_{E_i > 0} \langle \Phi_i | \Gamma | \Phi_i \rangle + \sum_{E_i = 0} \langle \Phi_i | \Gamma | \Phi_i \rangle. \tag{A149}$$

Due to the bijection established in Step 3, the states in the first sum occur in pairs of $(+1)$ and (-1). Therefore, the $E > 0$ sector strictly sums to zero, isolating the zero-energy vacuum sector. Defining n_B as the number of zero-energy bosons and n_F as the number of zero-energy fermions, the trace evaluates to

$$W = n_B - n_F. \tag{A150}$$

Tracing our explicit 6×6 fluid grading operator yields $W = -2$. The proof above requires that $n_B - n_F = -2$, guaranteeing the existence of at least two zero-energy vacuum states, $n_F \geq 2$.

In supersymmetric systems, dynamical breaking occurs if a continuous deformation of the physical parameters causes a zero-energy vacuum state to acquire a strictly positive energy. However, because W is a discrete topological invariant continuous variations cannot change its value. For a zero-energy state to acquire an excitation energy $E > 0$, it must ascend the energy spectrum alongside a degenerate superpartner of the opposite parity. Because $W = -2 \neq 0$ there is a strict numerical mismatch between bosonic and fermionic zero modes. The two unpaired fermionic zero-modes possess no available bosonic partners to form an $E > 0$ doublet. Therefore, dynamical supersymmetry breaking is mathematically forbidden.

Because the momentum-dependent grading operator Γ ensures that exact chiral symmetry is maintained globally this topological protection holds across the entire parameter space. By locking the unpaired zero-energy states in place the non-zero Witten index mathematically prohibits the steady-state geostrophic modes from acquiring non-zero propagating frequencies under continuous variations of planetary rotation.

Appendix C Supersymmetry in the Standard Complex-Valued Formulation of the Rotating Shallow Water Model

In the main text, we constructed a six-dimensional real Stueckelberg parameter space to identify the topological zero-modes of the rotating shallow water equations via the Witten index. It is instructive to demonstrate how this exact supersymmetric algebra manifests in the standard three-dimensional complex formulation of the fluid, which serves as the foundation for the quantum geometric tensor derivations by Ganeshan and Dorsey [10] and the topological band theory analysis by Delplace *et al.* [3].

In the standard complex formulation, the physical wave anomalies are represented by a three-component complex vector, $\Psi_C = (u, v, \eta)^{\mathrm{T}}$. The linearized equations of motion are cast as a local

 doi:10.20944/preprints202605.0606.v2

eigenvalue problem in momentum space, $\omega\Psi_C = \mathcal{H}_C\Psi_C$, where the 3×3 complex, self-adjoint Hamiltonian is given by

$$\mathcal{H}_C = \begin{pmatrix} 0 & if & k_x \\ -if & 0 & k_y \\ k_x & k_y & 0 \end{pmatrix}. \tag{A151}$$

Because this operator is self-adjoint,

$$\mathcal{H}_C^\dagger = \mathcal{H}_C, \tag{A152}$$

it fulfills the mathematical requirements of a fundamental supercharge in a supersymmetric algebra. We therefore identify the complex supercharge as

$$\mathcal{Q}_C \equiv \mathcal{H}_C. \tag{A153}$$

In standard supersymmetric quantum mechanics the energy must be non-negative. We generate the positive semi-definite supersymmetric Hamiltonian by squaring this supercharge,

$$\mathcal{H}_{\text{SUSY}}^{(C)} = \mathcal{Q}_C^2 = \begin{pmatrix} k_x^2 + f^2 & k_x k_y & -ifk_y \\ k_x k_y & k_y^2 + f^2 & ifk_x \\ ifk_y & -ifk_x & k^2 \end{pmatrix}. \tag{A154}$$

The eigenvalue spectrum of this operator is

$$E = \omega^2 \in \{0, k^2 + f^2, k^2 + f^2\}. \tag{A155}$$

This spectrum matches the unbroken supersymmetric requirement: an isolated zero-energy vacuum state situated below a set of doubly-degenerate excited supermultiplets (the high-frequency propagating Poincaré gravity waves).

To classify the spectrum topologically we introduce the 3×3 complex chiral grading operator, Γ_C. Following the physical Helmholtz decomposition established in our real formulation (Sec. 8) we partition the fluid based on the divergent and rotational components of the velocity field. Utilizing the momentum-dependent ratios $c = (k_x^2 - k_y^2)/k^2$ and $s = 2k_xk_y/k^2$, we define the grading matrix as

$$\Gamma_C = \begin{pmatrix} c & s & 0 \\ s & -c & 0 \\ 0 & 0 & -1 \end{pmatrix}. \tag{A156}$$

By construction, this operator evaluates the purely divergent velocity field as the bosonic sector (eigenvalue $+1$) and groups the rotational velocity field together with the scalar height anomaly η into the fermionic sector (eigenvalue -1).

This specific grading operator enforces exact chiral symmetry across the entire parameter space. Because the 2×2 velocity sub-block of Γ_C anticommutes with the 2×2 complex Coriolis sub-block $\begin{pmatrix} 0 & if \\ -if & 0 \end{pmatrix}$, the exact supersymmetric anticommutation relation holds irrespective of the planetary rotation rate,

$$\{\Gamma_C, \mathcal{Q}_C\} = 0, \quad \text{for all} \quad f. \tag{A157}$$

Because the chiral symmetry is exact, we evaluate the topological Witten index by taking the trace of the grading matrix,

$$W_C = \text{Tr}(\Gamma_C) = c - c - 1 = -1. \tag{A158}$$

The index $W_C = -1$ indicates the existence of $|W_C| = 1$ unbroken zero-energy mode, which corresponds to the single complex geostrophic zero-mode with $\omega(\boldsymbol{k}) = 0$, characteristic of the standard 3×3 shallow water system.

 doi:10.20944/preprints202605.0606.v2

This result highlights the mathematical correspondence between the standard complex geometry and the real Stueckelberg geometry. In the standard 3D complex formulation, the system is described by one complex zero-mode, $W_C = -1$, and one complex pair of excited bulk modes. By unpacking the complex phase into orthogonal $SO(2)$ quadratures the 6D real Stueckelberg formulation doubles the explicit degrees of freedom, and the Witten index accordingly doubles to $W = -2$, counting the independent real sine and cosine quadratures of the geostrophic balance. Whether analyzed via the 3D complex formulation or our 6D real formulation, the permanent existence of the zero-frequency geostrophic modes is a topologically protected consequence of unbroken supersymmetry.

Appendix D Geometric Interpretation of Topological Winding in Real Fluid Kinematics

To fully contextualize the topological arguments presented in this manuscript, it is instructive to review the mathematical foundations of winding numbers and how these abstract geometric invariants manifest in the macroscopic kinematics of classical real-valued fluids.

At its most fundamental mathematical level, a winding number is a discrete topological invariant that counts the total number of times a closed curve travels counterclockwise around a specific singular point, void, or origin within a given space. Because a closed path must ultimately return exactly to its starting coordinate, the total accumulated phase or angle must be an exact integer multiple of 2π. This strict quantization to integer values is the mechanism that endows topological systems with their characteristic robustness against continuous perturbations.

Appendix D.1 The One-Dimensional Mathematical Definition

Consider a closed continuous curve C in a two-dimensional plane, parameterized by a variable $t \in [0, 1]$ such that the start and end points are identical. If we track the polar angle $\theta(t)$ of the position vector as it traces this curve around a central origin, the winding number W_1 is defined as the total change in this angle integrated over the closed loop, normalized by a full rotation,

$$W_1 = \frac{1}{2\pi} \oint_C d\theta. \tag{A159}$$

If the curve completely circles the origin once in the counterclockwise direction, the integral evaluates to $W_1 = 1$. If the path circles twice in the clockwise direction, $W_1 = -2$. If the path does not enclose the origin at all, the accumulated angle naturally cancels out upon closing the loop, yielding $W_1 = 0$. In standard complex analysis, this geometric phase accumulation is elegantly formalized using a contour integral of a complex variable z around the origin, generating the argument principle,

$$W_1 = \frac{1}{2\pi i} \oint_C \frac{dz}{z}. \tag{A160}$$

The defining power of the winding number is its absolute topological protection via homotopy invariance. If one visualizes the closed curve as an elastic loop stretched around a fixed geometric obstacle, the loop can be subjected to continuous, arbitrary deformations—stretching, bending, or twisting—without altering the total number of times it encompasses the obstacle. So long as the loop is not broken (a discontinuous mapping) or forced directly through the singular origin (a topological phase transition), the integer winding number W_1 remains invariant. In physical systems, this guarantees that fundamental topological modes cannot be destroyed by smooth variations in parameters, material imperfections, or systemic noise.

Appendix D.2 Higher-Dimensional Winding and the Chern Number

The one-dimensional concept of a loop wrapping around a point in a plane described above generalizes naturally to higher-dimensional manifolds. In topological band theory, rather than analyzing a one-dimensional curve, we examine how a two-dimensional surface (such as the momentum

 doi:10.20944/preprints202605.0606.v2

space manifold parameterized by k_x and k_y) geometrically wraps around a singular point in a three-dimensional parameter space.

The mathematical machinery required to count this two-dimensional wrapping is the integration of the Berry curvature 2-form, Ω, over the closed manifold. The resulting discrete topological invariant is the Chern number, C, defined as

$$C = \frac{1}{2\pi} \iint \Omega_{k_x k_y} \, dk_x dk_y. \tag{A161}$$

Just as the one-dimensional winding number counts angular revolutions, the Chern number counts the quantized wrapping of the state vectors' internal geometric structure. In our rotating shallow water system, a calculated Chern number of $C = -2$ mathematically enforces that the geometric fiber bundle characterizing the fluid's parameter space entirely envelops the momentum-space singularity (the Dirac monopole) twice in a specified orientation.

Appendix D.3 Visualizing Continuous Degree-Two Topological Mappings

In geometric terms, $|C| = 2$ signifies that a two-dimensional parameter manifold (a sphere) continuously wraps around a central singularity exactly twice. Because human spatial intuition is conditioned by the mechanics of solid, impenetrable physical membranes, visualizing how a surface can envelop a solid volume twice without tearing or discontinuous overlapping is notoriously counter-intuitive. If one attempts to wrap a physical sheet around a sphere twice, the material must inevitably wrinkle, intersect itself, and create physical boundaries.

However, in topological band theory, the "surface" is not a physical membrane but a continuous mathematical mapping from a parameter space (the coordinates k_x, k_y) to a state space (the projective Hilbert space of the fluid). In this purely mathematical domain self-intersection does not violate continuity. To rigorously visualize this degree-two continuous mapping we provide three equivalent geometric models.

Appendix D.3.1 The Stretched Coordinate Mapping

The first visualization relies on an azimuthal coordinate transformation. Consider the standard parameter space of our fluid mapped onto a unit sphere, analogous to a geographic globe. We may slice this sphere along a single meridian from the North Pole to the South Pole and unroll it into a flat rectangular plane, mathematically equivalent to a Mercator projection. The left and right edges of this rectangle represent the exact same coordinate meridian.

Now, we apply a continuous scaling transformation to the azimuthal coordinate, stretching this rectangular domain horizontally until its width is doubled. We then map this stretched domain onto a target "state space" sphere. Because the parameter domain is twice as wide as the target's circumference, the surface wraps around the target sphere's equator exactly twice before the left and right edges meet to close the continuous manifold. Every single coordinate on the target sphere is now covered by exactly two layers of the parameter mapping.

This operation is perfectly continuous. No topological tears or discontinuous jumps occur at any point. At the poles, the mapping simply pivots around a single geometric coordinate twice. This demonstrates how a degree-two wrapping is achieved simply through a continuous linear scaling of the internal angular parameter.

Appendix D.3.2 The Complex Quadratic Mapping

A more formal mathematical visualization of this phenomenon is found in complex analysis via mapping the Riemann sphere. The Riemann sphere is a projection of the complex plane onto a three-dimensional globe, where the origin resides at the South Pole and spatial infinity converges at the North Pole.

 doi:10.20944/preprints202605.0606.v2

Consider the simple continuous complex function,

$$f(z) = z^2. \tag{A162}$$

In polar coordinates, a complex number is defined by a radius r and an azimuthal angle θ. The quadratic mapping transforms these coordinates via

$$(r, \theta) \mapsto (r^2, 2\theta). \tag{A163}$$

If we trace a continuous path along the equator of our starting parameter sphere, the initial angle traverses from $\theta = 0$ to $\theta = \pi$. Due to the 2θ multiplier in the mapping the corresponding image on the target sphere traverses from 0 to 2π, thereby completing one full revolution around the target equator.

As we complete the second half of our journey on the parameter sphere from $\theta = \pi$ to $\theta = 2\pi$, the image on the target sphere completes a second, entirely overlapping revolution from 2π to 4π. Because the quadratic function z^2 is everywhere smooth and infinitely differentiable, this double-layered mapping is continuous. The poles serve as topological branch points where the two continuous sheets merge.

Appendix D.3.3 The Degree-Two Vector Field

Finally, we can visualize this mapping by examining the continuous rotation of the fluid's eigenvector field in the momentum space parameter volume.

A standard degree-one topological monopole $|C| = 1$ can be visualized as a sphere covered in outward-pointing normal vectors (a "hedgehog" configuration). If an observer traverses the equator of this parameter sphere once, the local state vectors will sequentially tilt, completing one 360° rotation in the state space.

In contrast, our rotating fluid system is characterized by a degree-two monopole with $C = -2$. In this system the internal state vectors are highly twisted relative to the parameter coordinates. As an observer traverses the parameter equator by an angle ϕ, the fluid's eigenstate vectors rotate at an accelerated rate of 2ϕ. Consequently, by the time the observer has completed a single revolution around the parameter space, the internal vector field has continuously rotated through a full 720°.

If we map the directions of these state vectors onto a target unit sphere, the vectors will sweep across the entire surface of the target sphere exactly twice. The two distinct topological layers mapped over the sphere represent the continuous coexistence of the fluid's independent sine and cosine quadratures sharing the geometric parameter space.

Appendix D.4 Physical Interpretation of Quadrature Rotation and Double Winding

To rigorously define what is physically "rotating" in our real-variable topological model, one must examine the macroscopic fluid variables—zonal velocity u, meridional velocity v, and fluid height anomaly η—and analyze their spatial distribution in the physical domain.

In a standard complex formulation, a traveling wave is represented using the compact exponential $e^{i(\boldsymbol{k}\cdot\boldsymbol{x})}$. In the real-variable Stueckelberg formulation, we eschew the imaginary unit i and explicitly decompose the physical wave into its two fundamental spatial components: the cosine quadrature (the portion of the wave that is in-phase at the spatial origin) and the sine quadrature (the portion of the wave that is shifted by a quarter wavelength). Consequently, every physical field is expressed as a linear combination of these purely real, orthogonal standing wave patterns,

$$\begin{aligned} u(\boldsymbol{x}) &= u_c \cos(\boldsymbol{k}\cdot\boldsymbol{x}) + u_s \sin(\boldsymbol{k}\cdot\boldsymbol{x}), \\ v(\boldsymbol{x}) &= v_c \cos(\boldsymbol{k}\cdot\boldsymbol{x}) + v_s \sin(\boldsymbol{k}\cdot\boldsymbol{x}), \\ \eta(\boldsymbol{x}) &= \eta_c \cos(\boldsymbol{k}\cdot\boldsymbol{x}) + \eta_s \sin(\boldsymbol{k}\cdot\boldsymbol{x}). \end{aligned} \tag{A164}$$

 doi:10.20944/preprints202605.0606.v2

Our six-dimensional real state vector Φ is simply the ordered collection of these six macroscopic constant coefficients,

$$\Phi = \begin{pmatrix} u_c & v_c & \eta_c & u_s & v_s & \eta_s \end{pmatrix}^{\mathrm{T}}. \tag{A165}$$

In this formulation, the topological "winding" is not an abstract, unobservable complex phase; it is the continuous, systematic transfer of macroscopic wave amplitude back and forth between the cosine coefficients and the sine coefficients as the direction of the momentum wavevector $\boldsymbol{k}$ is continuously varied.

Consider a single propagating Poincaré mode. If we rotate the wavevector $\boldsymbol{k}$ in a closed circular path around the momentum origin by an azimuthal angle ϕ_k, the physical orientation of the wavecrests must continuously realign. At $\phi_k = 0$, a purely eastward propagating wave may have its zonal velocity perfectly aligned with the cosine quadrature, $u_c = 1, u_s = 0$. At this precise moment the maximum physical east-west surging of the fluid aligns exactly with the crests and troughs of the height anomaly.

As $\boldsymbol{k}$ is rotated through the parameter space, the changing geometric coordinates and the dynamical constraints of the Coriolis force necessitate a spatial phase shift. The wave energy smoothly drains out of the cosine quadrature component u_c and sloshes into the sine quadrature component u_s. When the energy has fully transferred such that $u_c = 0$ and $u_s = 1$, the maximum physical surging has shifted by exactly one quarter-wavelength in real physical space.

The antisymmetric complex structure operator, $\mathcal{J}$, serves as the exact mathematical generator for this continuous geometric transfer. It acts as a strict rotation matrix in the six-dimensional parameter space that systematically exchanges amplitude between the top three spatial components (u_c, v_c, η_c) and the bottom three spatial components (u_s, v_s, η_s). The topological winding is simply the observable, cyclic hand-off of this macroscopic wave energy.

Appendix D.5 The Origin of the $C = -2$ Topological Charge

To understand why this quadrature oscillation completes exactly two full cycles (a 4π or 720° phase rotation) during a single 2π rotation of the wavevector $\boldsymbol{k}$, one must recognize that fluid velocity is fundamentally a spatial vector field, behaving analogously to a spin-1 geometric system [10]. When the direction of propagation $\boldsymbol{k}$ is rotated by an angle ϕ_k, two distinct geometric and physical transformations occur simultaneously:

1. **Vector coordinate rotation:** Because the zonal and meridional velocities (u, v) form a two-dimensional spatial vector, the entire physical orientation of the fluid's velocity polarization ellipse must rotate in real space by ϕ_k simply to maintain its structural relationship with the new direction of the propagating wavevector.
2. **Coriolis precession:** The presence of the Coriolis parameter f breaks time-reversal symmetry, continuously exerting a perpendicular torque on the moving fluid. This induces an intrinsic kinematic precession of the velocity vector relative to the scalar height field η, effectively injecting an additional, structurally enforced phase shift of ϕ_k into the wave's internal geometry.

Because these two distinct geometric phenomena act in the same rotational orientation, they linearly superimpose. The physical fluid fields are structurally forced to cycle their energy between the cosine and sine quadratures twice as fast as the wavevector changes its global direction.

Consequently, by the time the wavevector $\boldsymbol{k}$ completes a single circumnavigation of the momentum origin the internal macroscopic wave amplitudes have executed a perfect double-cycle, mapping smoothly from $\cos \to \sin \to -\cos \to -\sin$, and then immediately repeating the sequence $\cos \to \sin \to -\cos \to -\sin$ a second time. This literal, observable re-allocation of physical kinetic and potential energy between the orthogonal spatial quadratures is the explicit geometric realization of the $C = -2$ topological monopole.

 doi:10.20944/preprints202605.0606.v2

Appendix D.6 Real-Variable Derivation of the Continuous Double-Winding in the Rotating Shallow Water System

To observe the topological double-winding within the real six-dimensional Stueckelberg formalism we begin with the normalized amplitude vector for the upper Poincare mode, P_1. Explicitly decomposed into its spatial cosine and sine quadratures $\Phi = (u_c, v_c, \eta_c, u_s, v_s, \eta_s)^{\mathrm{T}}$, and parameterized along a momentum-space circle of radius k_0 where $k_x = k_0 \cos\theta_k$ and $k_y = k_0 \sin\theta_k$, the raw vector is

$$\hat{\Phi}_{\mathrm{raw}}(\theta_k) = \frac{1}{\sqrt{2}} \begin{pmatrix} \cos\theta_k \\ \sin\theta_k \\ k_0/\omega \\ -(f/\omega)\sin\theta_k \\ (f/\omega)\cos\theta_k \\ 0 \end{pmatrix}. \tag{A166}$$

To uncover the global topological properties of this vector field, we must examine its behavior at the momentum origin $k_0 \to 0$, where the frequency $\omega \to f$. Formally taking this limit gives,

$$\hat{\Phi}_{\mathrm{raw}}(0) = \frac{1}{\sqrt{2}} \begin{pmatrix} \cos\theta_k \\ \sin\theta_k \\ 0 \\ -\sin\theta_k \\ \cos\theta_k \\ 0 \end{pmatrix}. \tag{A167}$$

Because the origin is a singular point with no directional dimension, a physically valid global section cannot retain any dependence on the azimuthal approach angle θ_k. The persistent θ_k dependence in $\hat{\Phi}_{\mathrm{raw}}(0)$ indicates a coordinate singularity, a topological vortex at the origin.

To remove this singularity and establish a smooth single-valued global state vector we must perform a continuous internal gauge transformation. In the real $\mathbb{R}^6$ formalism, this is accomplished by applying a rotation matrix $\mathcal{R}(\theta_k)$ generated by the antisymmetric complex structure operator $\mathcal{J}$. This rotation operator mixes the cosine and sine quadratures according to

$$\begin{pmatrix} \Psi_c' \\ \Psi_s' \end{pmatrix} = \mathcal{R}(\theta_k) \begin{pmatrix} \Psi_c \\ \Psi_s \end{pmatrix} = \begin{pmatrix} \cos\theta_k & -\sin\theta_k \\ \sin\theta_k & \cos\theta_k \end{pmatrix} \begin{pmatrix} \Psi_c \\ \Psi_s \end{pmatrix} = \begin{pmatrix} \Psi_c\cos\theta_k - \Psi_s\sin\theta_k \\ \Psi_c\sin\theta_k + \Psi_s\cos\theta_k \end{pmatrix} \equiv (\cos\theta_k + \mathcal{J}\sin\theta_k) \begin{pmatrix} \Psi_c \\ \Psi_s \end{pmatrix}. \tag{A168}$$

We now apply this rotational gauge transformation to our raw six-dimensional fluid state vector to generate the physically smooth state vector,

$$\hat{\Phi}_{\mathrm{smooth}} = \mathcal{R}(\theta_k)\hat{\Phi}_{\mathrm{raw}}. \tag{A169}$$

 doi:10.20944/preprints202605.0606.v2

Applying the standard trigonometric identities $\cos^2\theta_k = [1+\cos(2\theta_k)]/2$ and $\sin^2\theta_k = [1-\cos(2\theta_k)]/2$, after some algebra we find the smooth, analytically complete global section,

$$\begin{aligned} u'_c &= \frac{1}{2}\left(1+\frac{f}{\omega}\right)+\frac{1}{2}\left(1-\frac{f}{\omega}\right)\cos(2\theta_k), \\ v'_c &= \frac{1}{2}\left(1-\frac{f}{\omega}\right)\sin(2\theta_k), \\ \eta'_c &= \frac{k_0}{\omega}\cos\theta_k, \\ u'_s &= \frac{1}{2}\left(1-\frac{f}{\omega}\right)\sin(2\theta_k), \\ v'_s &= \frac{1}{2}\left(1+\frac{f}{\omega}\right)-\frac{1}{2}\left(1-\frac{f}{\omega}\right)\cos(2\theta_k), \\ \eta'_s &= \frac{k_0}{\omega}\sin\theta_k, \end{aligned} \tag{A170}$$

where the overall prefactor $1/\sqrt{2}$ has been dropped for notational simplicity. Notice that the emergence of the $2\theta_k$ argument is the direct, mathematically unavoidable consequence of applying the structure operator $\mathcal{J}$ to clear the coordinate singularity at the momentum origin. Consequently, as the fluid state traverses one 360° circle in parameter space, the scalar fluid height variables (η'_c, η'_s) execute *one* spatial cycle, while the internal macroscopic kinetic energy (u'_c, u'_s, v'_c, v'_s) sloshes between the independent sine and cosine quadratures *twice*, confirming the $C = -2$ topological invariant.

Notice also that at the momentum origin $k_0 \to 0$, where $\omega = f$, this smoothed global section yields a nice symmetric state vector,

$$\hat{\Phi}_{\text{smooth}}(0) = \frac{1}{\sqrt{2}}\begin{pmatrix}1 & 0 & 0 & 0 & 1 & 0\end{pmatrix}^{\mathrm{T}}, \tag{A171}$$

representing a perfect, equal superposition of the spatial cosine and sine quadratures, revealing the fundamental physical nature of the fluid at this limit. Since $u'_c = 1$ and $v'_s = 1$ (with all other components vanishing), the real-space macroscopic velocity fields simplify to

$$u(\boldsymbol{x}) = \frac{1}{\sqrt{2}}\cos(\boldsymbol{k}\cdot\boldsymbol{x}), \quad v(\boldsymbol{x}) = \frac{1}{\sqrt{2}}\sin(\boldsymbol{k}\cdot\boldsymbol{x}). \tag{A172}$$

Physically, this describes a wave where the zonal velocity u and the meridional velocity v possess identical amplitudes but are locked exactly 90° (a quarter-wavelength) out of phase with one another. In geophysical fluid dynamics, this configuration represents a pure, right-circularly polarized *inertial oscillation* driven entirely by the Coriolis force. Because the velocity vector sweeps out a perfect circle in physical space, the wave cannot favor one spatial quadrature over the other; it is structurally required to distribute its kinetic energy 50/50 between the sine and cosine. The $C = -2$ topological monopole is thus shown to be anchored by a highly symmetric, circularly polarized inertial state at its singular core.

Appendix D.7 Physical Manifestation in Real Planetary Fluids

In this paper we used the geometric framework described above to resolve the physical ambiguities raised by Biello and Dimofte [11] regarding the application of quantum topology to classical fluids. In standard quantum mechanics, winding numbers are traditionally derived from the rotating complex phase of a continuous probability wavefunction. The critics correctly observed that if classical macroscopic waves are real-valued linear combinations of these complex states, it must be explained why the topological winding phases do not simply cancel out through destructive interference upon superposition.

 doi:10.20944/preprints202605.0606.v2

Our $\mathbb{R}^6$ real parameter space formulation provides the explicit resolution. In the classical fluid, the "winding" is not an abstract, non-observable quantum phase factor. Instead, it is the genuine, measurable geometric rotation between the independent sine and cosine quadratures of the macroscopic fluid waves. This continuous rotation is generated and protected by the real antisymmetric complex structure operator, $\mathcal{J}$. Because the physical fluid basis vectors are mutually orthogonal in $\mathbb{R}^6$, their oriented wedge products do not mutually destruct. The winding phase is therefore a permanent, structural feature of the fluid's real symplectic kinematics.

Additionally, this bulk topological winding leads to the existence of the equatorial edge states via the bulk-boundary correspondence. If the bulk fluid parameter space possesses a non-zero structural winding with $C = -2$, any introduction of a physical boundary in real space (such as the equator where the Coriolis parameter f changes sign) forces this topologically protected twist to unravel. The mathematical mechanism by which the fluid resolves this boundary obstruction is by manifesting physical, localized edge states—the Kelvin and Yanai waves—that continuously bridge the topological gaps between the distinct bulk bands. Thus, the abstract winding number serves as a natural guarantee of the observable emergence of eastward-propagating weather patterns on a planetary scale.

Acknowledgments: The author thanks Alan Dorsey for introducing him to the fascinating topic of topological fluid dynamics.

References

1. B. A. Bernevig and T. L. Hughes, *Topological Insulators and Topological Superconductors* (Princeton University Press, 2013).
2. D. Vanderbilt, *Berry Phases in Electronic Structure Theory: Electric Polarization, Orbital Magnetization and Topological Insulators* (Cambridge University Press, 2018).
3. P. Delplace, J. B. Marston, and A. Venaille, Topological origin of equatorial waves, Science **358**, 1075–1077 (2017).
4. C. Tauber, P. Delplace, and A. Venaille, A bulk-interface correspondence for equatorial waves, J. Fluid Mech. **868**, R2 (2019).
5. N. Perez, A. Leclerc, G. Laibe, and P. Delplace, Topology of shallow-water waves on a rotating sphere, J. Fluid Mech. **1003**, A35 (2025).
6. T. Matsuno, Quasi-geostrophic motions in the equatorial area, J. Meteorol. Soc. Jpn. **44**, 25 (1966).
7. W. Thomson, On gravitational oscillations of rotating water, Proc. Royal Soc. Edinburgh **10**, 92–100 (1880).
8. R. Süsstrunk and S. D. Huber, Observation of phononic helical edge states in a mechanical topological insulator, Science **349**, 47 (2015).
9. L. M. Nash, D. Kleckner, A. Read, V. Vitelli, A. M. Turner, and W. T. M. Irvine, Topological mechanics of gyroscopic metamaterials, Proc. Natl. Acad. Sci. U.S.A. **112**, 14495 (2015).
10. S. Ganeshan and A. T. Dorsey, Quantum geometry of the rotating shallow water model, arXiv:2601.10695 [physics.flu-dyn].
11. J. A. Biello and T. Dimofte, Why do Earth's equatorial waves head east? Science **358**, 990–991 (2017).
12. E. C. G. Stueckelberg, Quantum Theory in Real Hilbert Space, Helv. Phys. Acta **33**, 727 (1960).
13. J. P. Provost and G. Vallee, Riemannian structure on manifolds of quantum states, Commun. Math. Phys. **76**, 289 (1980).
14. R. Cheng, Quantum Geometric Tensor (Fubini-Study Metric) in Simple Quantum System: A pedagogical Introduction, arXiv:1012.1337 [quant-ph].
15. N. Verma, P. J. W. Moll, T. Holder, and R. Queiroz, Quantum geometry and the hidden scales in materials, Nature Reviews Physics **8**, 226–239 (2026).
16. A. Gao, N. Nagaosa, N. Ni, and S.-Y. Xu, Quantum Geometry Phenomena in Condensed Matter Systems, arXiv:2508.00469 [cond-mat.str-el] (2025).
17. J. Yu, B. A. Bernevig, R. Queiroz, E. Rossi, P. Törmä, and B.-J. Yang, Quantum Geometry in Quantum Materials, arXiv:2501.00098 [cond-mat.mes-hall] (2025).
18. G. Fubini, Sulle metriche definite da una forma hermitiana, Atti del Reale Istituto Veneto di Scienze, Lettere ed Arti 63, 501 (1904).
19. E. Study, Kürzeste wege im komplexen gebiet, Math. Ann. 60, 321 (1905).
20. M. V. Berry, Quantal phase factors accompanying adiabatic changes, Proc. R. Soc. Lond. A **392**, 45 (1984).

 doi:10.20944/preprints202605.0606.v2

21. E. Witten, Dynamical breaking of supersymmetry, Nucl. Phys. B **188**, 513 (1981).
22. E. Witten, Constraints on Supersymmetry Breaking, Nucl. Phys. B **202**, 253 (1982).
23. L. E. Gendenshtein, I. V. Krive, Supersymmetry in quantum mechanics, Sov. Phys. Usp. **28**, 645–666 (1985).
24. F. Cooper, A. Khare, and U. Sukhatme, Supersymmetry and quantum mechanics, Phys. Rep. **251**, 267 (1995).
25. E. Gozzi, M. Reuter, and W. D. Thacker, Hidden BRS invariance in classical mechanics. II. Phys. Rev. D, **40**, 3363 (1989).
26. D. Tong, A Gauge Theory for Shallow Water, SciPost Phys. **14**, 102 (2023); arXiv:2209.10574 [hep-th]
27. A. Hatcher, Algebraic Topology (Cambridge University Press, 2002).
28. T. Needham, Visual Complex Analysis (Oxford University Press, 1997)
29. N. D. Mermin, The topological theory of defects in ordered media, Rev. Mod. Phys. **51**, 591—648 (1979).
30. G. K. Vallis, Atmospheric and Oceanic Fluid Dynamics: Fundamentals and Large Scale Applications (2nd ed.) (Cambridge University Press, 2017).
31. V. Zeitlin, Geophysical fluid dynamics: understanding (almost) everything with rotating shallow water models (Oxford University Press, 2018).